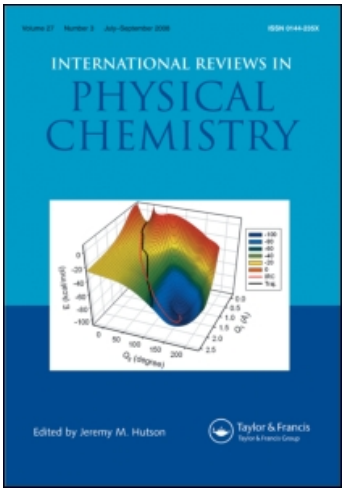

International Reviews in Physical Chemistry
Publication details, including instructions for authors and subscription information:
http://www.informaworld.com/smpp/title~content=t713724383

Stable icosahedral hollow cage clusters: stannaspherene () and plumbaspherene ()

Li-Feng Cui[a]; Lai-Sheng Wang
[a] Department of Physics, Washington State University, Richland, WA 99354

To cite this Article Cui, Li-Feng and Wang, Lai-Sheng(2008) 'Stable icosahedral hollow cage clusters: stannaspherene () and plumbaspherene ()', International Reviews in Physical Chemistry, 27: 1, 139 — 166
To link to this Article: DOI: 10.1080/01442350701791256
URL: http://dx.doi.org/10.1080/01442350701791256

International Reviews in Physical Chemistry
Vol. 27, No. 1, January–March 2008, 139–166

Taylor & Francis
Taylor & Francis Group

Stable icosahedral hollow cage clusters: stannaspherene (Sn_{12}^{2-}) and plumbaspherene (Pb_{12}^{2-})

Li-Feng Cui[a] and Lai-Sheng Wang[b]*

[a]*Department of Physics, Washington State University, 2710 University Drive, Richland, WA 99354;* [b]*Chemical & Materials Sciences Division, Pacific Northwest National Laboratory, MS K8-88, P. O. Box 999, Richland, WA 99352*

(*Received 30 October 2007; final version received 5 November 2007*)

One of the major objectives of cluster science is to discover stable atomic clusters, which may be used as building blocks for cluster-assembled nanomaterials. The discovery and bulk synthesis of the fullerenes have sprouted new research disciplines in chemistry and nanoscience and precipitated intense interest to search for other similar stable clusters. However, despite major research efforts, no other analogous gas-phase clusters have been found and yielded to bulk syntheses. In this article, we review our recent discoveries in cluster beam experiments of stannaspherene (Sn_{12}^{2-}) and plumbaspherene (Pb_{12}^{2-}), which are highly stable and symmetric cage clusters. The names for these two clusters derive from their icosahedral (I_h) symmetry and delocalized spherical π-bonding that are characteristics of buckminsterfullerene C_{60}. Stannaspherene and plumbaspherene have diameters comparable to that of C_{60} and can be considered as inorganic analogues of the buckyball. The large internal space in Sn_{12}^{2-} has been shown to be able to trap any transition metal atom to form new endohedral cage clusters, $M@Sn_{12}^{2-}$, analogous to endohedral fullerenes. The doped atom in $M@Sn_{12}^{2-}$ keeps its quasi-atomic nature with large magnetic moments. These endohedral cages form a rich class of new building blocks for cluster-assembled materials with tunable magnetic, electronic, and chemical properties. During our attempt to synthesize endohedral stannaspherenes, we crystallized a new $Pd_2@Sn_{18}^{4-}$ cluster, which can be viewed as the fusion of two $Pd@Sn_{12}^{2-}$ clusters. This result suggests that stannaspherene, plumbaspherene, and a large number of their endohedrally doped species can be synthesized in the bulk.

Keywords: stannaspherene; plumbaspherene; cage clusters; photoelectron spectroscopy; tin clusters

Contents

*Corresponding author. Email: ls.wang@pnl.gov

ISSN 0144–235X print/ISSN 1366–591X online

DOI: 10.1080/01442350701791256
http://www.informaworld.com

1. Introduction

Clusters are aggregates of atoms intermediate between individual atoms and bulk matter. In the size regime from a few to a few hundred atoms, the chemical and physical properties of clusters exhibit dramatic atom-by-atom size dependences, forming the foundation for nanoscience. The quest for novel physically and chemically stable clusters that are promising for cluster-assembled nanomaterials has been one of the major goals of cluster science. The discovery of C_{60} in cluster beam experiments and its subsequent bulk synthesis have heightened research efforts in this area.[1,2] Experimental and computational advances have now made it possible to elucidate detailed structures and chemical bonding for fairly complicated cluster systems. Recent discoveries, such as the all-metal aromatic clusters,[3,4] planar and tubular boron clusters,[5–8] novel planar, pyramidal, and hollow-cage gold clusters,[9–13] and special Al and Al hydride clusters,[14–16] demonstrate that cluster science remains a very active and exciting field of study.

Since the discovery of the fullerenes, there has been intense interest in hollow cage clusters, particularly in the heavy congeners of carbon – Si and Ge. However, small Si and Ge clusters seem to exhibit tetrahedral bonding features,[17–44] very different from those of carbon clusters. For example, the obvious valence isoelectronic Si_{60} cluster does not have the same structure as C_{60}.[45,46] Instead of a beautiful soccer-ball shape, Si_{60} seems to adopt a rather low-symmetry structure.[46] Elongated structures have been found for small Si and Ge clusters of dozens of atoms,[32–36] while more compact structures have been proposed for larger ones. The growth pattern of tin clusters has also been suggested to resemble those of Ge and Si clusters on the basis of ion mobility measurements.[47,48] Thus, it was quite a

surprise when we observed a unique photoelectron spectrum for Sn_{12}^-, which led to the discovery of a tin cage cluster.[49]

In this article, we review the serendipitous discovery of the cage cluster Sn_{12}^{2-} (stannaspherene)[49] and the related Pb_{12}^{2-} (plumbaspherene) cluster,[50] which possess icosahedral structures and delocalized spherical π-bonding. These highly symmetric hollow cages have sizes comparable to that of C_{60} and can be viewed as inorganic analogues of the fullerenes. More interestingly, these two cages can entrap a foreign atom to form endohedral cage clusters, analogous to the endohedral fullerenes. A series of endohedral stannaspherenes $M@Sn_{12}^{2-}$, with M = transition metals including the f-block elements, have been produced and investigated.[51] The doped atom in $M@Sn_{12}^{2-}$ has been shown to keep its quasi-atomic nature with large magnetic moments if M = transition metals with an open d- or f-shell. These endohedral stannaspherenes yield a rich class of new building blocks for cluster-assembled materials with potentially tunable magnetic, electronic, and chemical properties. During our attempt to synthesize the endohedral stannaspherene, we have crystallized a new $Pd_2@Sn_{18}^{4-}$ cluster, which can be viewed as the fusion of two $Pd@Sn_{12}^{2-}$ clusters,[52] suggesting that stannaspherene, plumbaspherene, and their endohedral species can be synthesized in bulk.

2. Experimental method

In our laboratory, photoelectron spectroscopy (PES) of size-selected anions, often in combination with *ab initio* calculations, is used to probe the electronic and geometrical structures and chemical bonding of gas-phase atomic clusters.[53–56] We chose cluster anions for experimental PES studies for two primary reasons: (1) anions allow size-selection with mass spectrometry; and (2) PES of anions yields spectroscopic information for neutral clusters, which are of most interest. Experiments are carried out using a magnetic-bottle time-of-flight photoelectron spectrometer, details of which have been described previously.[57] Figure 1 shows a schematic of our magnetic-bottle PES apparatus with a laser vaporization supersonic cluster source. Cluster anions are produced by laser vaporization of a disk target with a helium carrier gas and analysed using a time-of-flight mass spectrometer. Clusters of interest are mass selected by a three-grid mass gate and decelerated before crossing with a detachment laser beam in the interaction zone of the magnetic-bottle photoelectron analyser. Several different detachment photon energies are usually used, ranging from the second to fourth harmonics of a Nd:YAG laser (532, 355, 266 nm), to 193 and 157 nm from an excimer laser.

We have found that cluster temperatures play the most critical role in determining the quality of PES spectra using the laser vaporization cluster sources.[58] Nascent clusters can be quite hot due to the heat of formation and for negatively charged clusters the electron affinities. We observed that with our source configuration well-resolved PES spectra can be obtained by carefully selecting those clusters that have sufficient resident time in the nozzle to be thermalized.[59] Clusters with short resident time in the nozzle are relatively hot, which usually yield poorly resolved PES spectra. Photoelectrons are collected at nearly 100% efficiency by the magnetic bottle and analysed in a 3.5-m-long electron flight tube. Electron binding energy spectra are obtained by subtracting the kinetic energy spectra from the photon energies of the detachment laser. The spectra are calibrated using the

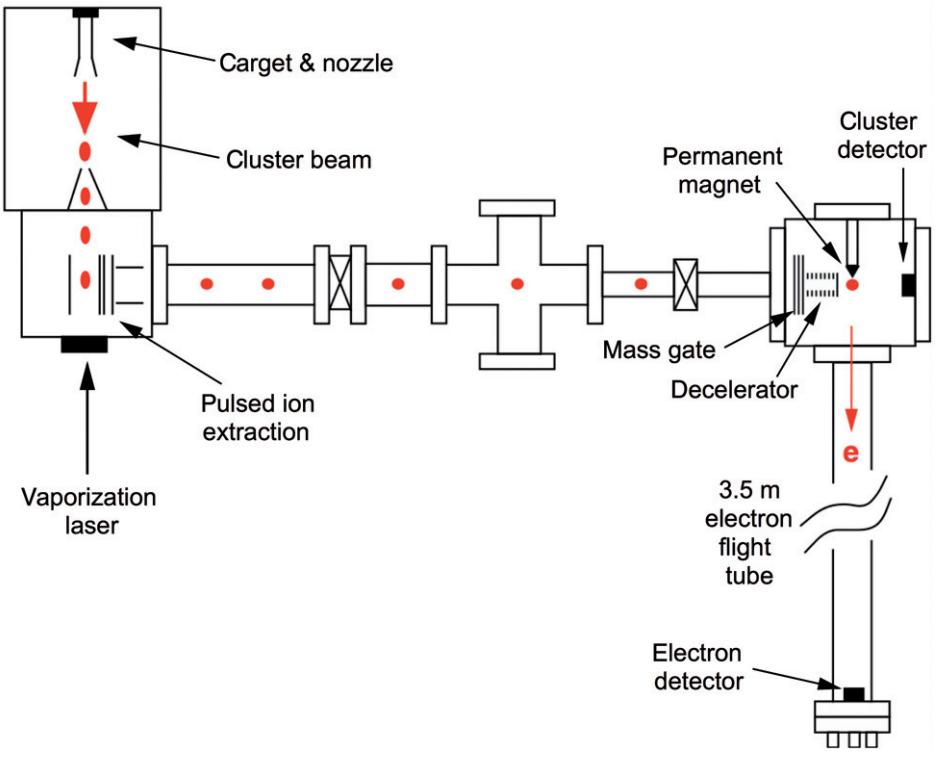

Figure 1. Schematic view of the magnetic-bottle photoelectron apparatus with a laser vaporization supersonic cluster source.

known spectra of atomic anions, such as Cu^-, Rh^-, Au^- or Pt^-. The apparatus has an electron energy resolution of $\Delta E/E \approx 2.5\%$, i.e. about 25 meV for 1 eV electrons.

3. Stannaspherene and plumbaspherene

3.1. *The unique PES spectral pattern of* Sn_{12}^-

Different from its lighter congeners, silicon and germanium which are semiconductors, the normal allotrope of tin under ambient conditions (β-Sn) is a metal with a body-centred tetragonal lattice, but it also has a small band gap semiconducting phase (α-Sn) with a diamond lattice similar to Si and Ge that is stable at low temperatures.[60] Prior experimental[47,61–64] and theoretical[65–68] studies have suggested that small tin clusters possess similar structures to those of Si and Ge. An interesting experimental observation is that small tin clusters exhibit melting temperatures exceeding that of the bulk,[61] consistent with the notion that small tin clusters have similar bonding configurations as those of the semiconductor Si and Ge clusters. Previous PES experiments[69–71] also suggested that the spectra of small Sn_n^- clusters are similar to those of the corresponding Ge_n^- clusters. However, these PES experiments were all done at low photon energies ($\leq$4.6 eV) and under relatively low resolutions.

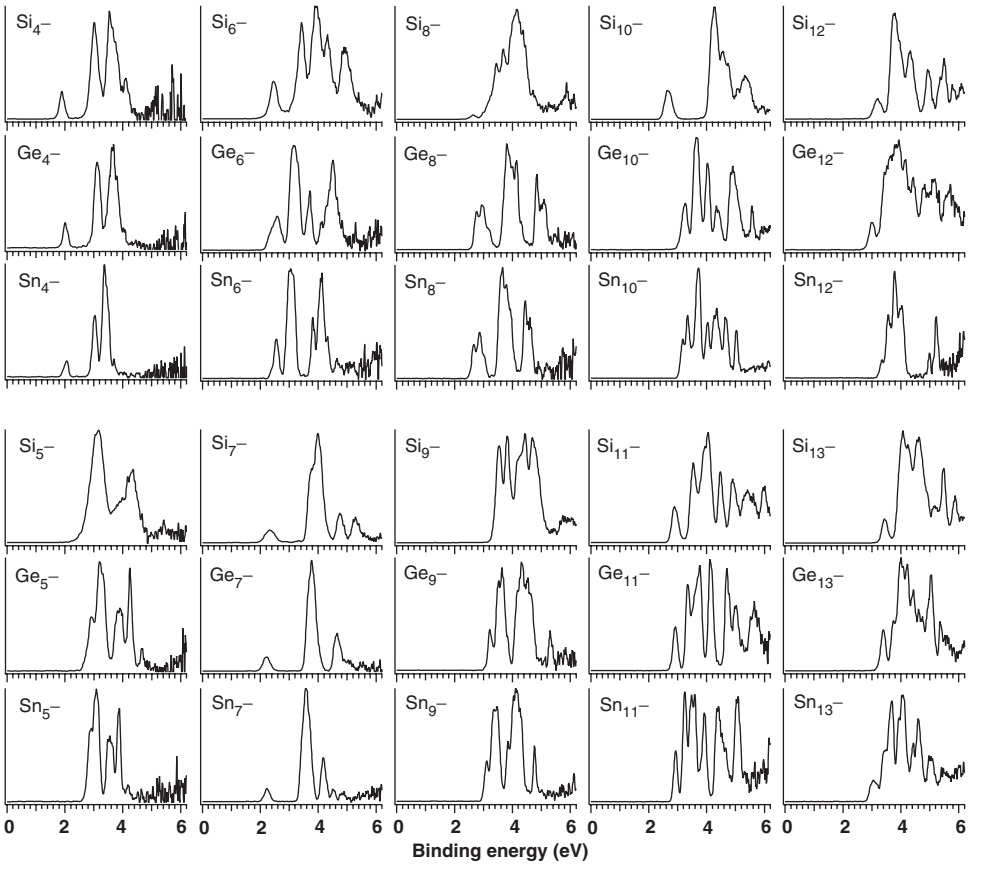

Figure 2. Photoelectron spectra of Sn_n^- ($n = 4$–13) at 193 nm compared to those of Si_n^- and Ge_n^-. From ref. 72.

Bulk tin is a metal under ambient condition, whereas the structures and bonding of small Sn clusters have been suggested to be semiconductor-like. So there must be a semiconductor-to-metal transition for Sn clusters as a function of size. We carried out a PES study to probe the electronic structure evolution of Sn_n^- clusters, in particular, the semiconductor-to-metal transition, at a higher photon energy (193 nm: 6.424 eV) and improved spectral resolution.[72] The obtained PES spectra revealed a distinct semiconductor-to-metal transition for Sn_n clusters at $n = 42$. More importantly, our well resolved PES spectra at the high photon energy immediately enabled us to recognize the remarkably simple spectrum of Sn_{12}^-, leading to the discovery of stannaspherene.[49]

Figure 2 shows the PES spectra of Sn_n^- ($n = 4$–13) compared with those of the corresponding Si_n^- and Ge_n^- clusters. For all the clusters in this size range (except $n = 12$), the spectra of Sn_n^- are similar to those of Ge_n^-, suggesting they possess similar geometrical structures. However, the spectrum of Sn_{12}^- is very different from the spectrum of Ge_{12}^- or other Sn_n^- clusters in the similar size range. Whereas the spectrum of Sn_{12}^- is rather congested with numerous poorly resolved features, that of Sn_{12}^- is very simple and

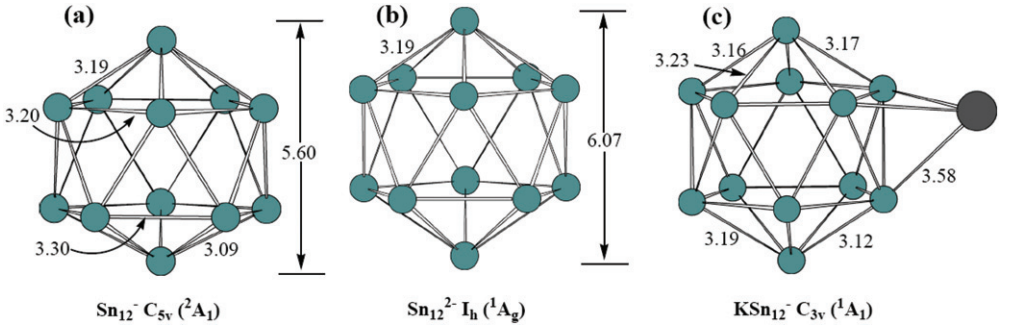

Figure 3. Optimized structures of (a) Sn_{12}^-; (b) Sn_{12}^{2-}; (c) KSn_{12}^-. The bond distances and cage diameters are in Å. From ref. 49.

well-structured. Four bands were resolved in the binding energy range from 3 to 4 eV, followed by a large gap and two well-resolved bands around 5 eV. The lowest energy band yielded an adiabatic detachment energy, i.e. the electron affinity of neutral Sn_{12}, to be 3.23 ± 0.05 eV and a vertical detachment energy (VDE) of 3.34 ± 0.03 eV. Although low-symmetry structures similar to Ge_{12} have been proposed for Sn_{12}, the relatively simple and characteristic PES spectrum of Sn_{12}^- immediately suggested that it should possess a high-symmetry structure different from that of Ge_{12}^-.

3.2. *Structures of* Sn_{12}^- *and* Sn_{12}^{2-}

In search for the possible high-symmetry structures for Sn_{12}^-, we started from the highest symmetry possible for a twelve-atom cluster – an icosahedral cage. However, the Jahn–Teller effect led to a slightly lower symmetry C_{5v} ($^2A_1$) species (Figure 3a), which is only slightly distorted from the I_h structure mainly by the depression of one apex atom. The computed first VDE (3.27 eV) of the C_{5v} Sn_{12}^- is in excellent agreement with the experimental value of 3.34 eV. By adding one electron to Sn_{12}^-, we found that the resulting Sn_{12}^{2-} species is a highly stable I_h cage with a closed electron shell (Figure 3b). Several other low-symmetry structures, including those suggested for Ge_{12}, have also been calculated for Sn_{12}^{2-}, but they are all much higher in energy (Figure 4). We were able to produce Sn_{12}^{2-} in the form of KSn_{12}^- ($K^+[Sn_{12}^{2-}]$) experimentally by laser vaporization of a tin target containing ~15% K. The photoelectron spectrum of KSn_{12}^- (Figure 5b) is very similar to that of Sn_{12}^-, suggesting that the Sn_{12}^{2-} motif is not distorted greatly due to the presence of K^+. Our calculations showed that the K^+ counter ion is outside the Sn_{12}^{2-} cage with a C_{3v} ($^1A_1$) symmetry (Figure 3c). Indeed, only relatively small structural perturbations are observed in the Sn_{12}^{2-} cage due to the K^+ coordination. The isomer with K^+ inside the Sn_{12}^{2-} cage is much higher in energy by 3.4 eV because of the large size of the K^+ ion, which expands the cage diameter from 6.07 Å (Figure 3b) to ~6.45 Å.

3.3. *The chemical bonding in* Sn_{12}^{2-}

To help understand the stability and chemical bonding of the I_h-Sn_{12}^{2-} cage, we performed a detailed analysis of its valence molecular orbitals. Sn has a valence electron configuration

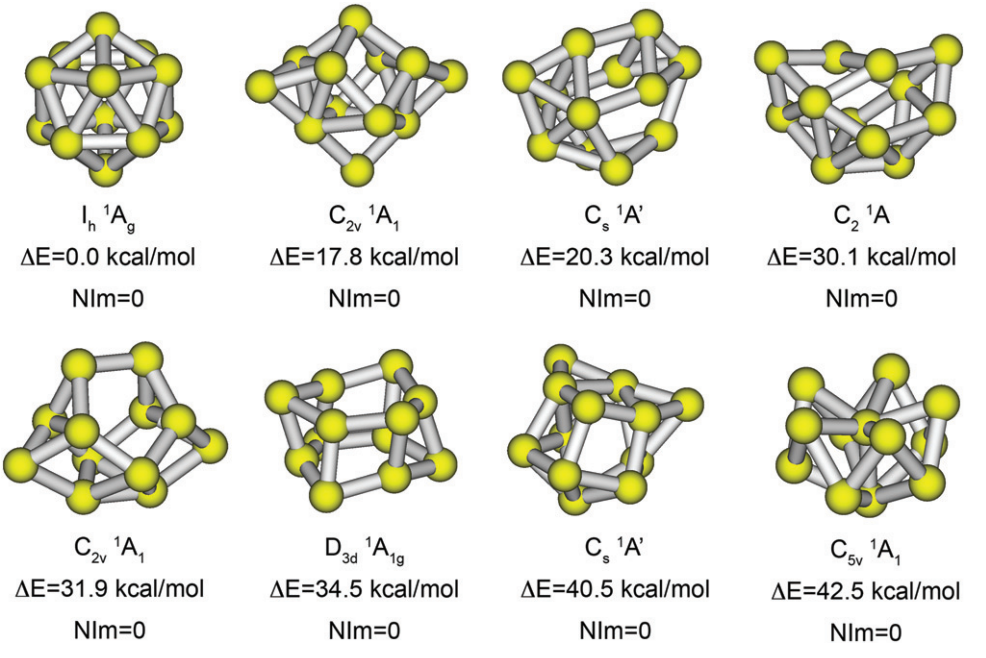

Figure 4. Alternative structures of Sn_{12}^{2-}. The energies are relative to the I_h cage. All structures are local minima calculated using Gaussion 03 at the B3LYP/3-21G level of theory. From ref. 49.

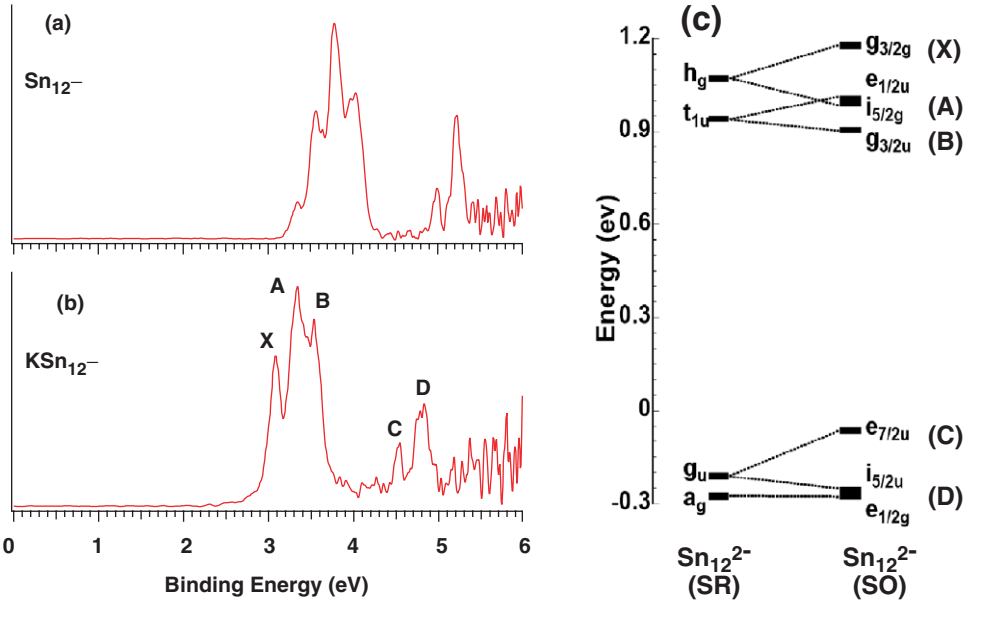

Figure 5. Photoelectron spectra of (a) Sn_{12}^- and (b) KSn_{12}^- at 193 nm. (c) Scalar relativistic (SR) energy levels of the 5p-based valence molecular orbitals of the I_h Sn_{12}^{2-} and the correlation to the spin–orbit (SO) coupled levels of I_h^* Sn_{12}^{2-}, where the asterisk indicates the double-group symmetry. From ref. 49.

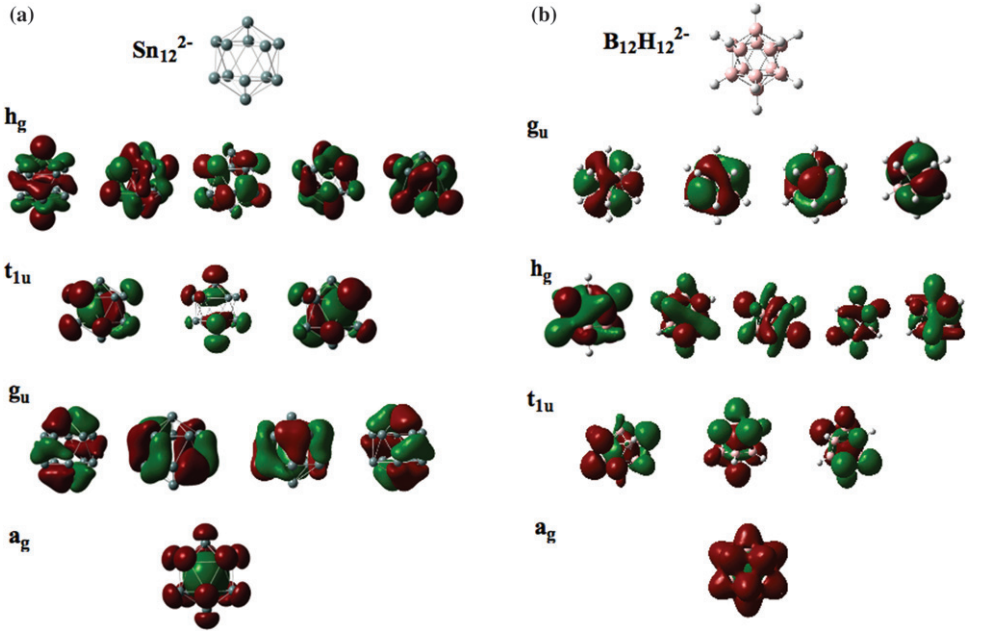

Figure 6. Comparison of the valence molecular orbitals of (a) Sn_{12}^{2-} and (b) $B_{12}H_{12}^{2-}$. From ref. 49.

of $5s^25p^2$. Because of the large energy separation between the 5s and 5p shells there is little s-p hybridization in the Sn_{12}^{2-} cage; the $5s^2$ electron pair is largely localized on each Sn atom, leaving only the two 5p electrons participating in the bonding on the Sn_{12}^{2-} cage. Figure 5c shows the valence molecular orbital diagram at the scalar relativistic (SR) and spin–orbit (SO) coupled levels. It is shown that the MO levels of Sn_{12}^{2-} with SO effect are in excellent agreement with the PES spectral pattern of $K^+[Sn_{12}^{2-}]$: the observed spectral features (X, A, B, C, D) are labeled in Figure 5c next to the SO levels.

Among the 13 valence molecular orbitals, four are delocalized radial π bonding orbitals (a_g and t_{1u}) formed from the radial p_z atomic orbitals. The remaining nine orbitals (g_u and h_g) are delocalized in-sphere σ bonding orbitals from the tangential p_x and p_y atomic orbitals. The bonding pattern in Sn_{12}^{2-} is remarkably similar to that in the well-known *closo*-borane molecule $B_{12}H_{12}^{2-}$ (Figure 6), which was first predicted to be a stable molecule by molecular orbital theory[73] and subsequently synthesized.[74] The B_{12} cage framework in $B_{12}H_{12}^{2-}$ is also bonded similarly by four delocalized radial π bonding orbitals and nine in-sphere delocalized σ orbitals with 12 localized B-H bonds, which are equivalent to the $5s^2$ electrons in the Sn_{12}^{2-} cage. Because of the delocalized π bonding in Sn_{12}^{2-} and its spherical symmetry, a name, stannaspherene, is coined for this highly stable and symmetric species.

3.4. Pb_{12}^{2-}: *plumbaspherene*

Bulk lead is a metal like tin. In addition, because of the relativistic effect[75] the 6s electron pair in lead is expected to be even more inert and lead clusters should be primarily bonded

by the 6p electrons. Thus, we expect that Pb_{12}^{2-} should also be a highly stable cage like Sn_{12}^{2-}. We obtained the 193 nm PES spectra of Pb_n^- clusters and observed that the spectrum of Pb_{12}^- is special, similar to that of Sn_{12}^{2-}. We found that Pb_{12}^{2-} is indeed a highly stable I_h cage,[50] which has an even larger interior volume than stannaspherene. A disk of pure lead was used as the laser vaporization target to produce the Pb_n^- clusters. For the Pb_{12}^{2-} experiment, a lead target containing ~15% potassium was used and the Pb_{12}^{2-} cage was produced in the form of KPb_{12}^-, i.e. $K^+[Pb_{12}^{2-}]$.

3.4.1. *PES spectra of pure and doped lead clusters*

Figure 7 displays the PES spectra of Pb_n^- ($n = 11$–13) at 193 nm. Clearly, the Pb_{12}^- spectrum is special relative to those of its neighbours, showing only four bands (X, A, B, C), whereas much more complex spectral features are observed for Pb_{11}^- and Pb_{13}^-. This observation suggests that Pb_{12}^- should possess a relatively high-symmetry structure. We also obtained the spectrum of Pb_{12}^- at 266 nm, which is compared to the 193 nm spectrum in Figure 8, as well as to the corresponding spectra of KPb_{12}^-. The 355 nm spectrum of Pb_{12}^- (not shown) can only access the first detachment feature (X) around 3.1 eV. At 266 nm, the A and B bands of Pb_{12}^- between 3.5 and 4 eV are resolved into at least five spectral features. The spectra of KPb_{12}^- are nearly identical to those of Pb_{12}^- (Figure 8), except that they are shifted to lower binding energies due to charge transfer from K to the Pb_{12} moiety, $K^+[Pb_{12}^{2-}]$. At 266 nm, the first band (X) of KPb_{12}^- at 2.7 eV is resolved into a doublet, whereas a shoulder on the lower binding energy side is resolved in the B band at ~3.6 eV. The weak continuous signals beyond 5 eV in the 193 nm spectra for both Pb_{12}^- and KPb_{12}^- are due to a combination of imperfect background subtraction and possible multi-electron processes (shake-up processes). The electron affinities of Pb_{12} and KPb_{12} are measured from the threshold feature to be 3.09 ± 0.03 and 2.71 ± 0.03 eV, respectively. The vertical detachment energies for the ground state transitions for Pb_{12}^- and KPb_{12}^- are measured to be 3.14 ± 0.03 and 2.77 ± 0.03 eV, respectively. The PES spectra of Pb_{12}^- and other small Pb_n^- clusters have been measured previously at lower spectral resolution and lower photon energies.[69,71] The current experiment yielded better resolved spectra, more accurate electron binding energies, and more spectral features to cover the valence spectral range.

3.4.2. *Structure and bonding of Pb_{12}^- and Pb_{12}^{2-}*

Geometry optimization for Pb_{12}^- from a high-symmetry icosahedral cage led to a Jahn–Teller distorted lower symmetry C_{5v} species (Figure 9a), analogous to Sn_{12}^- (Section 3.2.). The computed first vertical detachment energy (3.08 eV) of the C_{5v} Pb_{12}^- is in excellent agreement with the experimental value of 3.14 eV. Whereas ion mobility experiment suggests that Pb_n^+ clusters possess compact near-spherical structures,[48] several theoretical studies have given various structures for neutral Pb_{12}.[76–79] Two recent works by Wang *et al.*[78] and Rajesh *et al.*[79] suggest distorted cage structures for Pb_{12}. However, we found that the doubly charged Pb_{12}^{2-} species is a highly stable and perfect I_h cage with a closed electron shell (Figure 9b). We were able to generate Pb_{12}^{2-} stabilized by a counter ion in KPb_{12}^- ($K^+[Pb_{12}^{2-}]$), whose PES spectra are compared to those of Pb_{12}^- in Figure 8. The similar PES spectra between KPb_{12}^- and Pb_{12}^- suggest that the Pb_{12}^{2-} cage upon K^+ coordination is probably not distorted too much from the

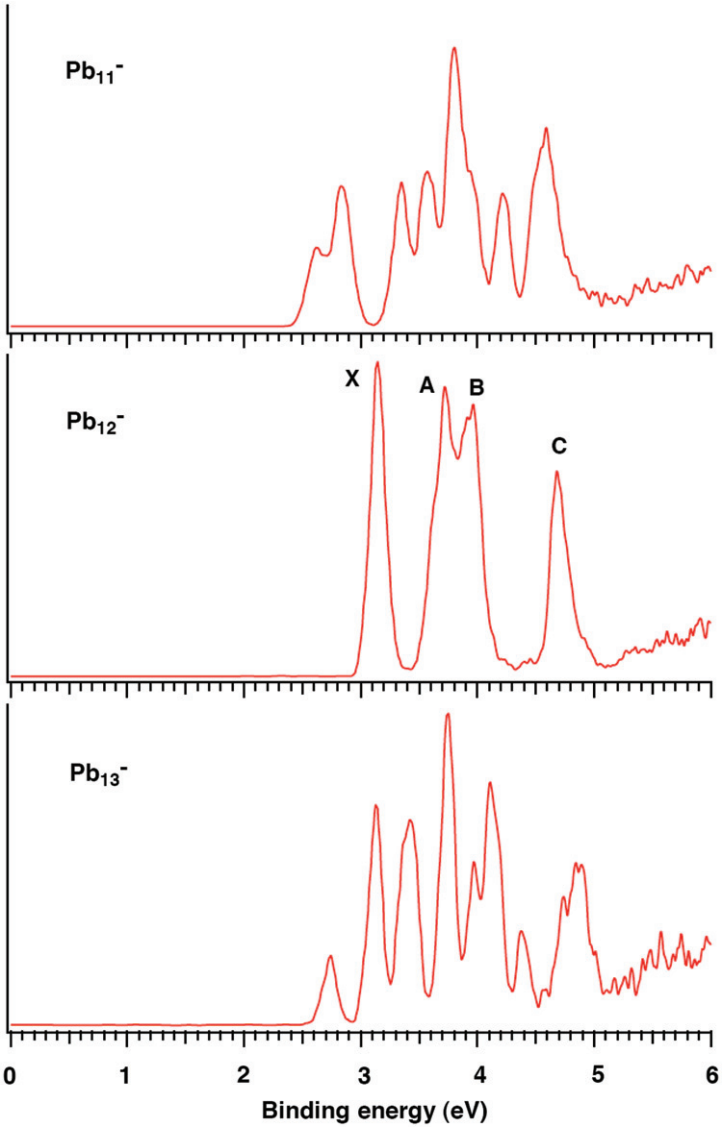

Figure 7. Photoelectron spectra of Pb_n^- ($n = 11$–13) at 193 nm. Note the relatively simple spectral pattern of Pb_{12}^- with respect to those of Pb_{11}^- and Pb_{13}^-. From ref. 50.

ideal I_h symmetry, which is borne out from our calculated structure (Figure 9c). Our calculations showed that the K^+ counter ion prefers to stay outside the cage with a C_{3v} ($^1A_1$) symmetry, inducing very little perturbation to the Pb_{12}^{2-} cage relative to the ideal I_h symmetry. The isomer with K^+ inside the Pb_{12}^{2-} cage is much higher in energy by 2.37 eV because of the large size of the K^+ ion. The calculated vertical detachment energy (2.78 eV) of the C_{3v} KPb_{12}^- agrees very

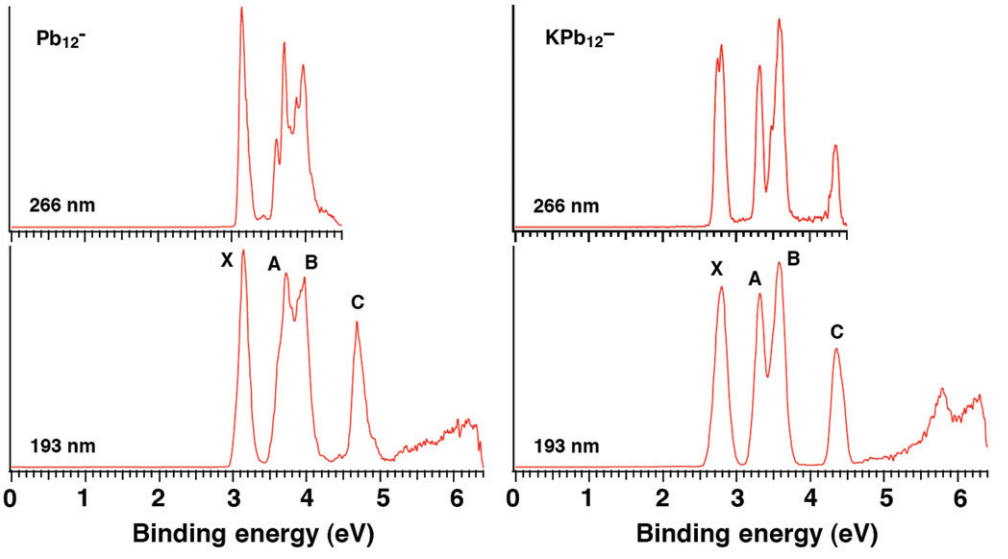

Figure 8. Photoelectron spectra of Pb_{12}^- at 266 and 193 nm compared to those of KPb_{12}^-. From ref. 50.

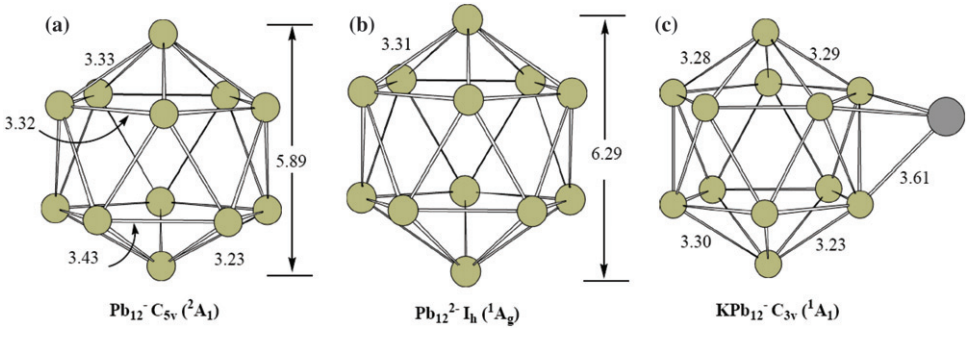

Figure 9. Optimized structures for (a) Pb_{12}^-, (b) Pb_{12}^{2-}, (c) KPb_{12}^-. The bond distances and cage diameters are in Å. From ref. 50.

well with the experimental value of 2.77 eV, lending considerable credence to the identification of the I_h Pb_{12}^{2-} cage.

The PES spectra of both Pb_{12}^- and KPb_{12}^- can be understood from the valence molecular orbitals of the I_h Pb_{12}^{2-}, as shown in Figure 10. Under the I_h symmetry, the 6p-based valence orbitals of Pb transform into MOs t_{1u}, h_g, g_u, and a_g in Pb_{12}^{2-}, which form two groups with a large energy gap at the scalar relativistic level of theory (Figure 10). The 6s-based MOs are much more stable due to the so-called 'inert electron pair effect' arising from the relativistic effects[75]; they are separated by more than 4 eV from the 6p-based MOs and cannot be accessed even at 193 nm in our PES experiments for Pb_{12}^- and KPb_{12}^-. However, when spin–orbit coupling effect, which is expected to be very large for Pb, is considered, the orbital pattern becomes quite different (Figure 10). The strong SO

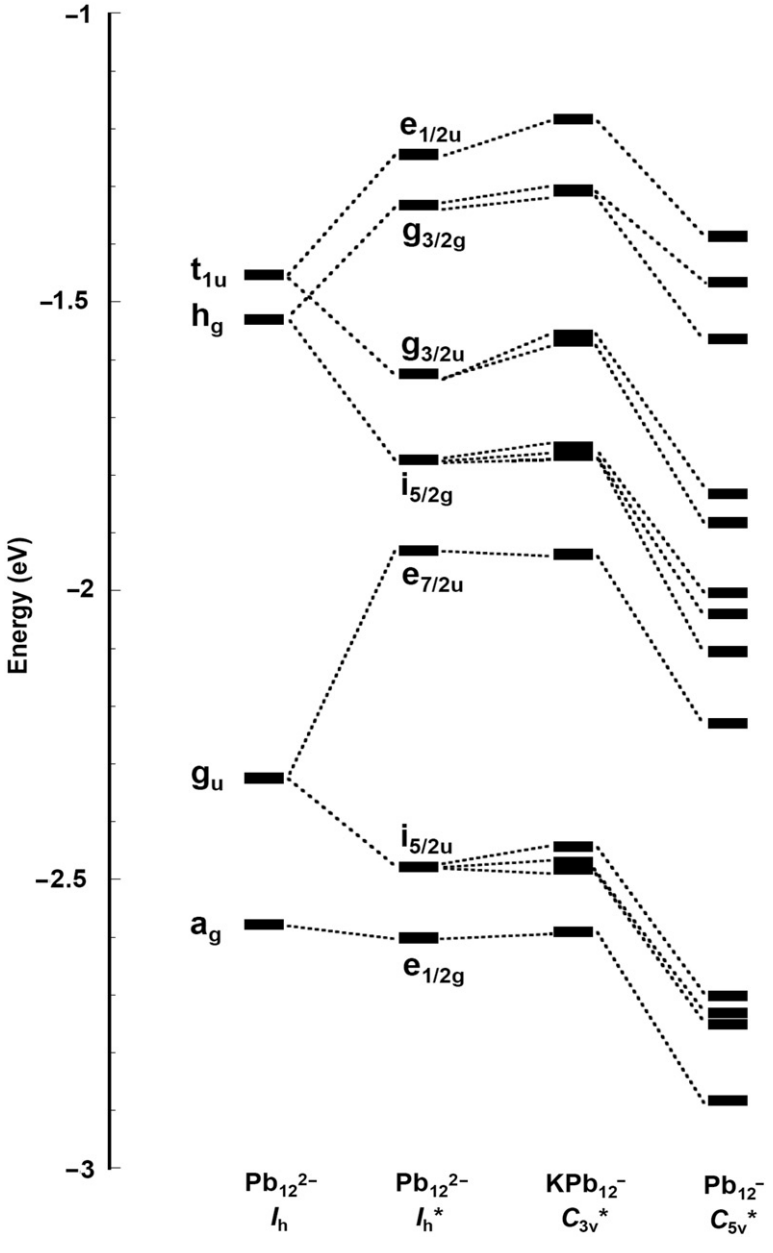

Figure 10. Scalar relativistic (SR) energy levels of the 6p-based valence MOs of the I_h Pb_{12}^{2-} and the correlation to the spin-orbit coupled levels of I_h^* Pb_{12}^{2-} and the lower symmetry C_{3v}^* $K^+[Pb_{12}^{2-}]$ and C_{5v}^* Pb_{12}^- (the asterisk indicates the double-group symmetry). The 6s-based MOs are mainly localized on each atom and are separated from the bottom of the 6p band by more than 4 eV. The energy levels of Pb_{12}^{2-} are shifted down by 2.63 eV to compare with the monoanions. From ref. 50.

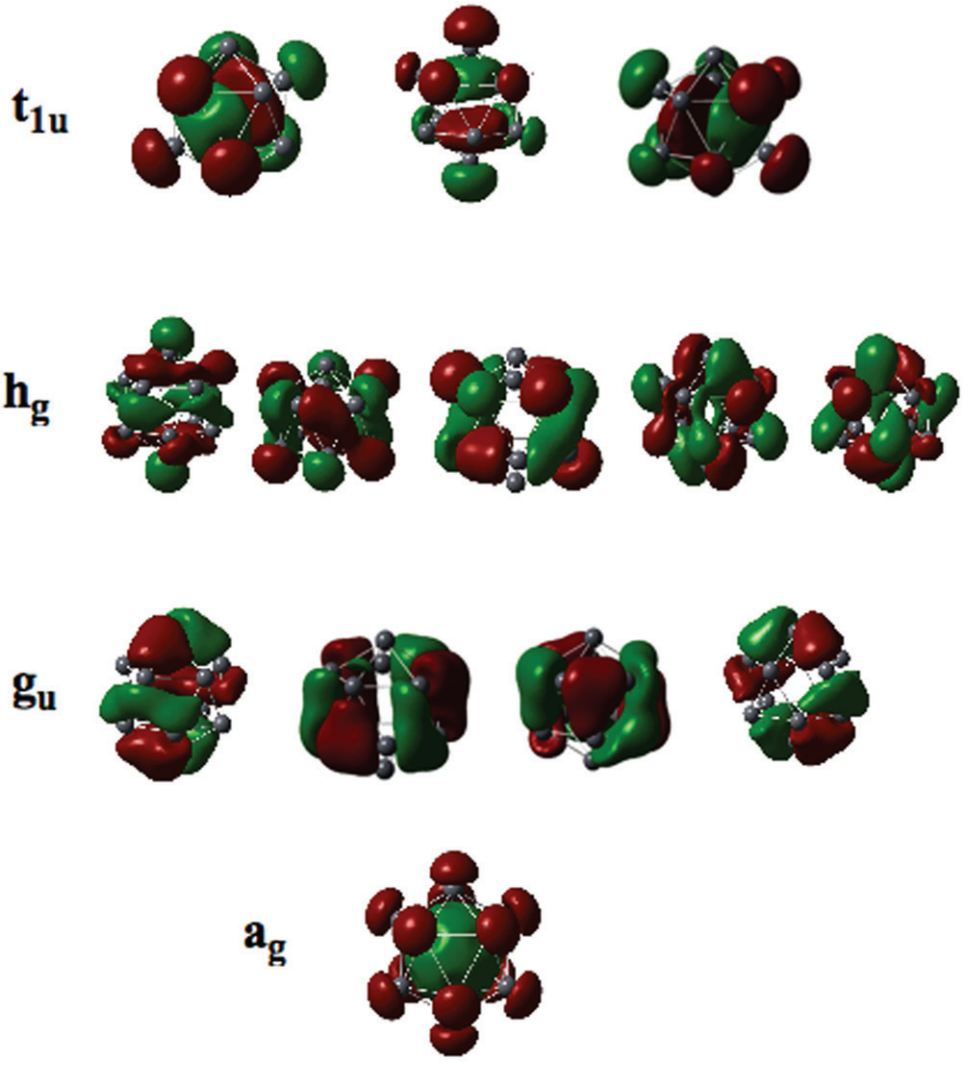

Figure 11. Pictures of the valence molecular orbitals of Pb_{12}^{2-}. From ref. 50.

coupling transforms the MOs into three groups of energetically separated spinors: ($e_{1/2u}$, $g_{3/2g}$), ($g_{3/2u}$, $i_{5/2g}$, $e_{7/2u}$), and ($i_{5/2u}$, $e_{1/2g}$). This pattern of spinors is in remarkable qualitative agreement with the observed PES spectra for Pb_{12}^{-} and KPb_{12}^{-}, suggesting that further splittings of the MOs in the lower symmetry Pb_{12}^{-} and KPb_{12}^{-} are relatively small. This is indeed the case, as illustrated in the energy correlation diagrams in Figure 10. The small energy splitting is a result of the relatively small structural distortions from the I_h structure in Pb_{12}^{-} and KPb_{12}^{-}, indicating the structural robustness of the 12 atom Pb cage.

The canonical scalar-relativistic MOs of Pb_{12}^{2-} shown in Figure 11 are similar to those of the stannaspherene Sn_{12}^{2-}, which has been shown to be valent isoelectronic to the $B_{12}H_{12}^{2-}$ molecule (Figure 6). Among the 13 valence MOs, there are four radial π orbitals (a_g and

t_{1u}) and nine in-sphere σ MOs (g_u and h_g). Analogous to Sn_{12}^{2-}, which has been named as stannaspherene for its π bonding character and its nearly spherical structure,[49] we suggest 'plumbaspherene' for the highly stable and robust Pb_{12}^{2-} cage.

Plumbaspherene has a computed diameter of 6.29 Å, slightly larger than that of stannaspherene (6.07 Å). Thus, it is expected that Pb_{12}^{2-} can trap an atom inside to form endohedral plumbaspherene, $M@Pb_{12}$. This is indeed the case and will be discussed more latter (see Section 6).

4. Endohedral stannaspherenes

The large interior volumes of stannaspherene and plumbaspherene suggest that they may trap a foreign atom to form new endohedral clusters, analogous to the endohedral fullerenes. We have carried out an extensive experimental and theoretical search for endohedral stannaspherenes. We have produced Sn_{12}^- clusters doped with one transition metal atom, (MSn_{12}^-) throughout the transition metal series (M = Ti, V, Cr, Fe, Co, Ni, Cu, Au, Pt, Nb, Ta, Hf, Y, Gd) by laser vaporization of pressed Sn/M disk targets and obtained their PES spectra.[51] Both experimental and theoretical evidence shows that all the transition metal atoms are endohedrally doped ($M@Sn_{12}^-$) and they maintain perfect or pseudo-icosahedral symmetry with the central atom inducing very little distortion to the Sn_{12}^{2-} cage. More interestingly, the central atom in $M@Sn_{12}^-$ maintains its quasi-atomic nature analogous to that in the endohedral fullerenes,[80,81] yielding a rich class of potential building blocks for new materials with tunable electronic, magnetic, or chemical properties.

4.1. *PES spectra of M@Sn_{12}^-*

Figure 12 displays the 193 nm PES spectra of Sn_{12}^- doped with 3d transition metals and a few selected 4d and 5d dopants. More spectra with other dopants including rare earth elements are given in Figure 13. All the spectra are well resolved with numerous distinct electronic transitions. In general, the spectra of $M@Sn_{12}^-$ become more complicated as one moves from Cu to the left of the transition series due to the open d shell and the relative orbital-energy variation of the 3d electrons, which are core-like in Cu, but become frontier levels in the early transition metals. Remarkably, there is a characteristic doublet feature around 5 eV (labeled g_u in Figure 12), which is present in all the spectra with little variation among the different doped $M@Sn_{12}^-$ species. This spectral feature provides the key experimental evidence for the endohedral nature of all the doped clusters and is important to compare with theoretical calculations.

4.2. *Structures and bonding of Cu@Sn_{12}^- and Au@Sn_{12}^-*

The doublet spectral feature around 5 eV in all the $M@Sn_{12}^-$ clusters (Figures 12 and 13) bears considerable resemblance to similar spectral features primarily derived from the on-sphere g_u σ orbitals in stannaspherene (see Figure 5), suggesting that all the doped $M@Sn_{12}^-$ clusters possess similar electronic structures and that the Sn_{12} cage is intact in $M@Sn_{12}^-$. To confirm the endohedral nature of $M@Sn_{12}^-$ and understand their electronic structure, we performed extensive theoretical calculations. We first focused on the $CuSn_{12}^-$

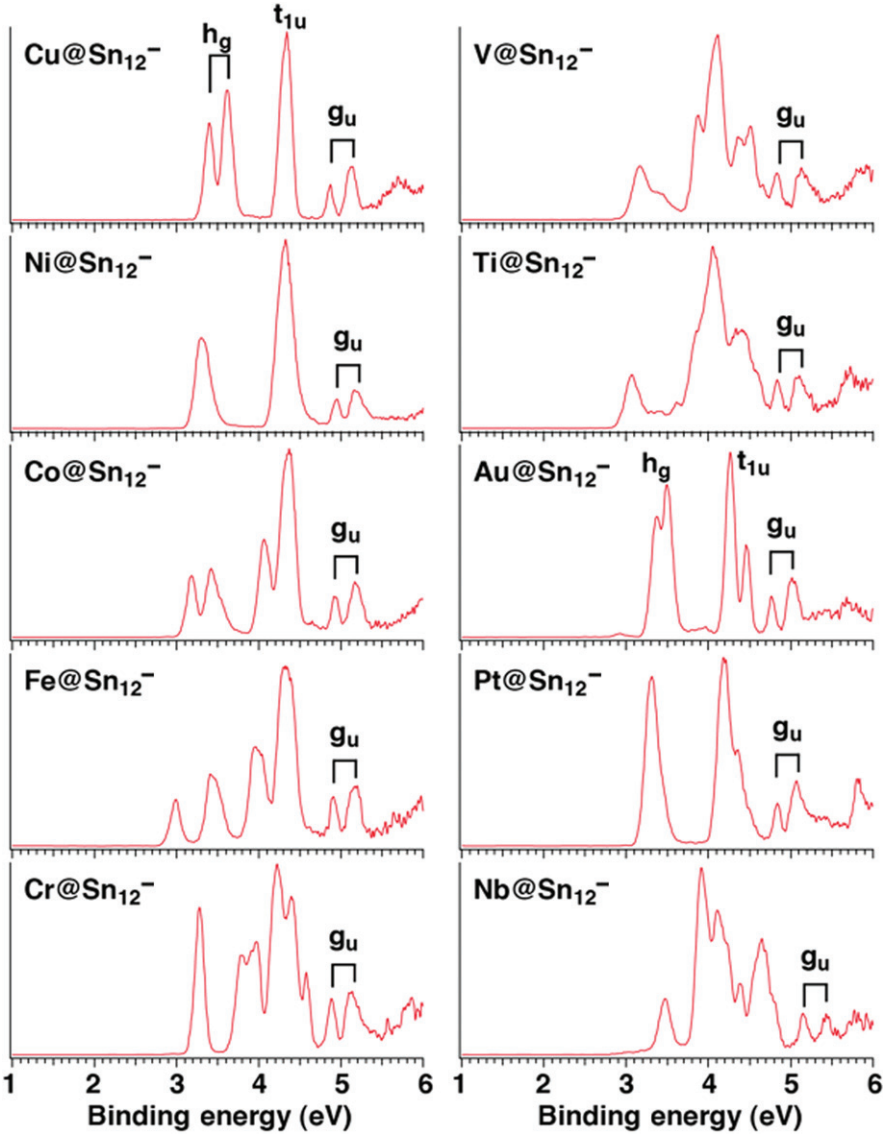

Figure 12. Photoelectron spectra of $M@Sn_{12}^{2-}$ (M = Cu, Ni, Co, Fe, Cr, V, Ti, Au, Pt, Nb) at 193 nm. From ref. 51.

system because it possesses a closed-shell electronic structure. Figure 14 displays the structure of the endohedral $Cu@Sn_{12}^{-}$ compared to those of several exohedral structures. The theoretical results indicate that indeed the endohedral $Cu@Sn_{12}^{-}$ is overwhelmingly more stable than any of the exohedral isomers. The calculated adiabatic and vertical detachment energies and simulated photoelectron spectrum of the endohedral $Cu@Sn_{12}^{-}$ with spin–orbit coupling are in excellent agreement with the experimental data (Figure 15), confirming unequivocally its stability and structure.

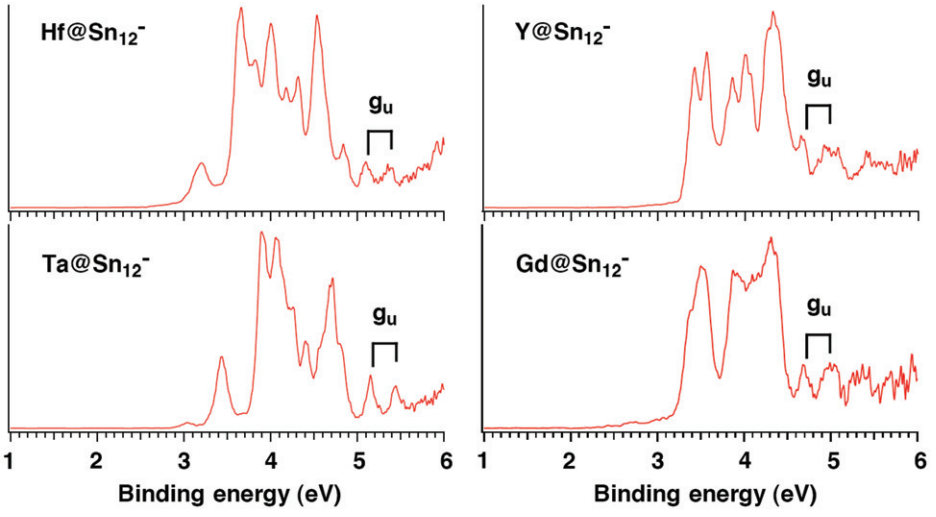

Figure 13. Photoelectron spectra of more endohedral stannaspherenes $M@Sn_{12}^-$ (M = Hf, Ta, Y, Gd) at 193 nm. From ref. 51.

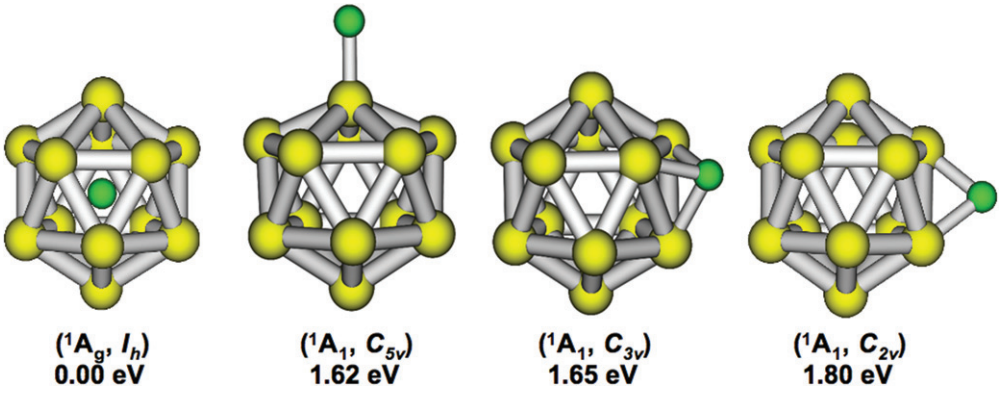

Figure 14. Optimized structures of the global minimum endohedral $Cu@Sn_{12}^-$ cluster and several exohedral $CuSn_{12}^-$ and their relative energies at B3LYP level of theory.[51]

$Cu@Sn_{12}^-$ is a perfect icosahedral cluster (Figure 14) with a Sn–Sn distance (3.21 Å), very close to that in stannaspherene (3.19 Å), suggesting moderate interactions between the central Cu atom and the Sn_{12} cage. The Cu-Sn distance (3.05 Å) in $Cu@Sn_{12}^-$ is considerably longer than the Cu–Sn distance (2.6 Å) in diatomic CuSn,[82] consistent with the relatively weak covalent interactions between Cu and the Sn_{12} cage in $Cu@Sn_{12}^-$. In fact, $Cu@Sn_{12}^-$ can be described as a Cu^+ ion trapped inside stannaspherene, $Cu^+@Sn_{12}^{2-}$, similar to the charge transfer complexes formed in endohedral fullerenes.[83] Figure 16 compares the scalar relativistic and spin–orbit coupled energy levels of the valence molecular orbitals of $Cu@Sn_{12}^-$ and those of stannaspherene. As shown above,

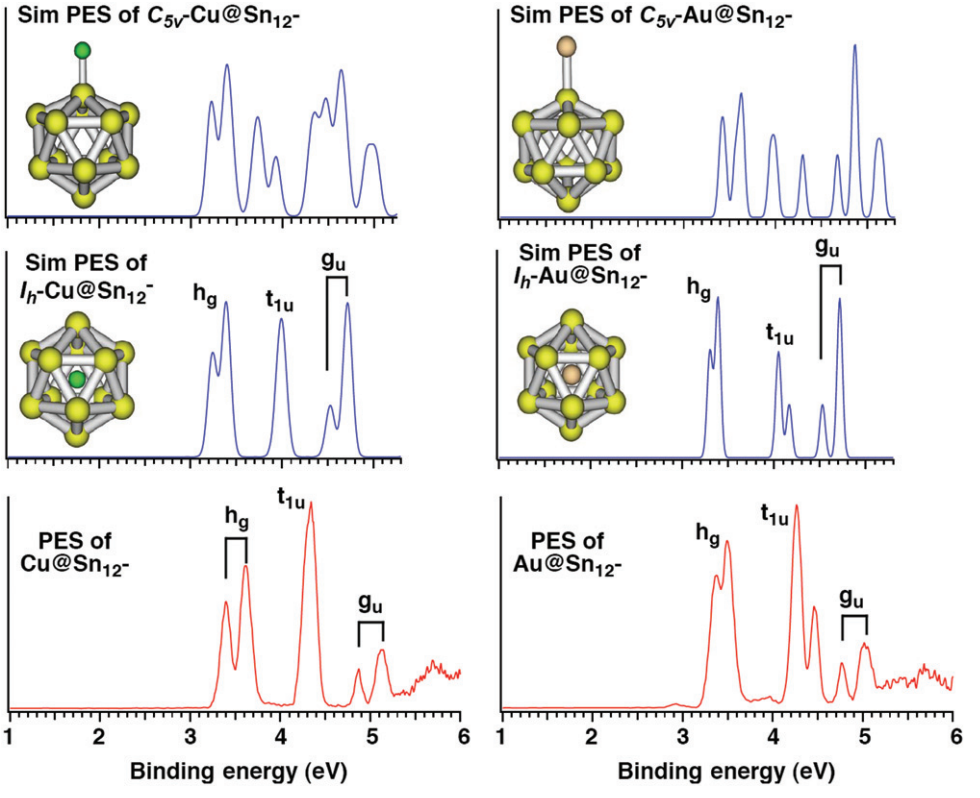

Figure 15. Comparison of the simulated spectra of the endohedral I_h Cu@Sn_{12}^- and Au@Sn_{12}^-, and the exohedral C_{5v} $CuSn_{12}^-$ and $AuSn_{12}^-$ to the respective experimental photoelectron spectra. Note the dramatic difference between the simulated spectra for the global minima I_h endohedral cages and the C_{5v} exohedral isomers. The simulated spectra were obtained simply by fitting calculated spin–orbital energies with gaussion functions, whereas the intensities were not calculated explicitly.[51]

stannaspherene is bonded by the Sn 5p electrons only, which transform into h_g, t_{1u}, g_u, and a_g valence MOs (Figure 6), whereas the Sn 5s electrons are mainly non-bonding lone pairs. Upon insertion of Cu^+ into Sn_{12}^{2-}, the radial bonding MOs (a_g and t_{1u}) are stabilized because they are symmetry-allowed to interact with the d orbitals of the dopant, whereas the purely tangential g_u MO is not affected at all because of symmetry restrictions, as shown in Figure 16. The h_g HOMO, which has a small amount of mixing from the radial orbitals is slightly destabilized. The filled $3d^{10}$ shell of Cu transforms into an h_g orbital in $Cu^+@Sn_{12}^{2-}$, maintaining its fivefold degeneracy. When spin–orbit coupling is taken into account, each degenerate orbital is split into two levels. The SO coupling in the corresponding MOs in Cu@Sn_{12}^- and Sn_{12}^{2-} are very similar (Figure 16). The spin–orbit split MO pattern of Cu@Sn_{12}^- is in excellent agreement with the observed PES spectral pattern, as labeled in the spectrum of Cu@Sn_{12}^- (Figure 12). The Cu $3d^{10}$ levels and the a_g orbital have too high binding energies to be ionized at the photon energy used. The spin–orbit splittings in the h_g HOMO and the g_u orbitals are large enough to be clearly resolved experimentally. The spectrum of Au@Sn_{12}^- is almost identical to that of Cu@Sn_{12}^- except

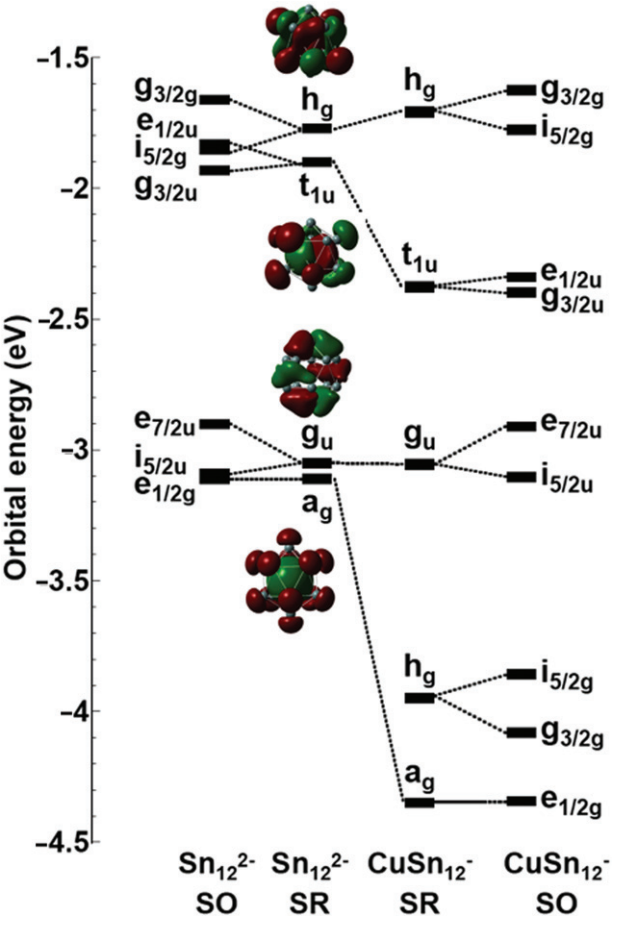

Figure 16. Correlation diagram between the scalar relativistic (SR) valence levels of Sn_{12}^{2-} and $Cu@Sn_{12}^{-}$ and their spin-orbit split levels. The SR molecular orbital contour surfaces of Sn_{12}^{2-} are also shown. The lower h_g orbital in $Cu@Sn_{12}^{-}$ is the Cu $3d^{10}$ shell. From ref. 51.

that the spin–orbit splitting in the t_{1u} orbital is enhanced in $Au@Sn_{12}^{-}$, which is also borne out from our calculations (Figure 15), confirming the endohedral nature of $Au@Sn_{12}^{-}$. The first ADE and VDE of $Cu@Sn_{12}^{-}$ and $Au@Sn_{12}^{-}$ are very similar, as seen from the PES spectra (Figure 15).

4.3. *Structures and bonding of* $M@Sn_{12}^{-}$ *with open-shell 3d dopants*

Although the $Cu@Sn_{12}^{-}$ cluster possesses perfect icosahedral symmetry, our calculations show that the other endohedral $M@Sn_{12}^{-}$ clusters with open d shells on the central dopants except $Cr@Sn_{12}^{-}$ (Figure 17) have slightly distorted structures. However, the structural distortions are very small and the actual cage structure of all the $M@Sn_{12}^{-}$ clusters are very close to the ideal I_h symmetry. The nearly identical doublet features around 5 eV in all the

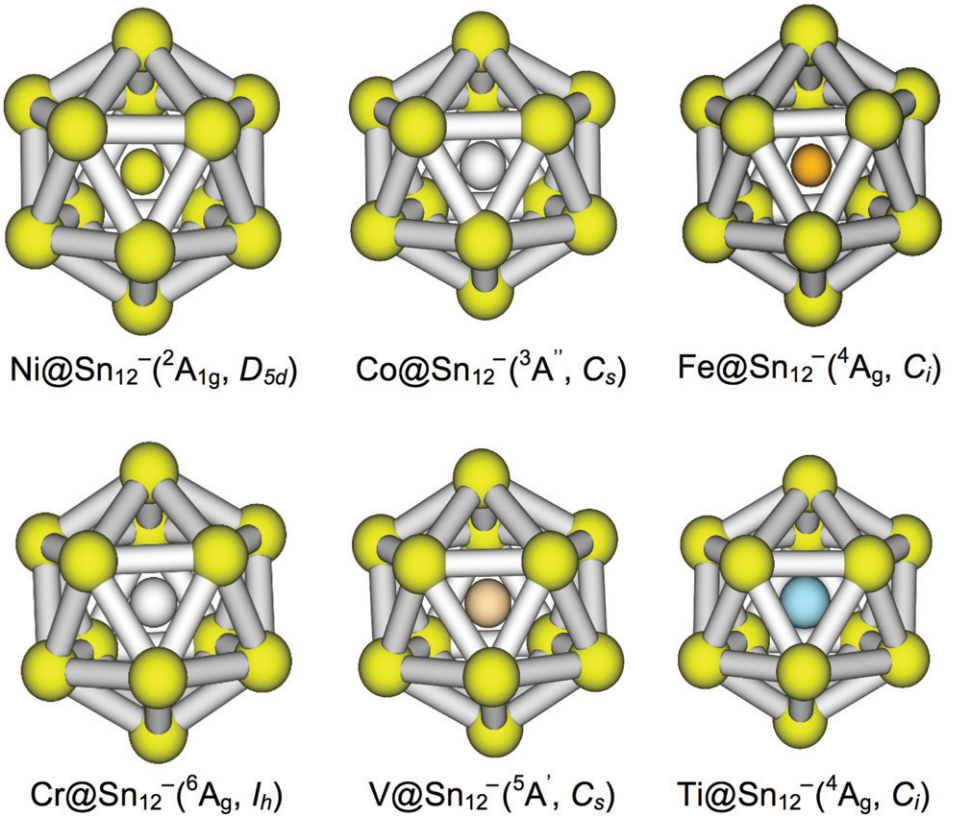

Figure 17. Optimized structures of the endohedral stannaspherenes $M@Sn_{12}^-$ with open shell 3d endohedral atoms (M = Ni, Co, Fe, Cr, V, and Ti). From ref. 51.

spectra of the $M@Sn_{12}^-$ clusters are due to the same g_u orbitals (Figure 12), which are purely on-sphere σ orbitals (Figure 16) and are not expected to be affected by the central atom. This spectral characteristic provides a fingerprint for the endohedral cage structures for all the $M@Sn_{12}^-$ clusters and reflects the robustness of the stannaspherene cage. The more complicated spectral features in the lower binding energy range in the open d-shell $M@Sn_{12}^-$ clusters are expected. For the late transition metal dopants (Ni, Fe, Co), our calculations show that the 3d electrons are still significantly lower in energy and cannot be detached at 193 nm. The extra spectral features in $Co@Sn_{12}^-$ and $Fe@Sn_{12}^-$ are likely due to spin polarization of the h_g HOMO and the t_{1u} orbitals. For the early transition metal dopants (Cr, V, Ti), the 3d electrons have similar binding energies as the Sn-derived frontier h_g and t_{1u} orbitals, resulting in much more complex spectral patterns due to direct detachment from the 3d valence levels in the low binding energy region (Figure 12). The 4d and 5d dopants behave similarly as the 3d dopants, resulting in similar PES spectra for the corresponding endohedral stannaspherenes. Our photoelectron spectra suggest that the rare-earth atoms also form endohedral stannaspherenes, judged by the g_u doublet spectral fingerprint in the spectra of $Y@Sn_{12}^-$ and $Gd@Sn_{12}^-$ (Figure 13) and confirmed by our theoretical calculations.

All the $M@Sn_{12}^-$ anionic species can be described as $[M^+@Sn_{12}^{2-}]$, whereas the neutral endohedral stannaspherenes ($M@Sn_{12}$) can be described as $[M^{2+}@Sn_{12}^{2-}]$. For the 3d dopants, all the endohedral stannaspherenes are magnetic with high spins, characteristic of the atomic 3d electrons ranging from $3d^2$ in $[Ti^{2+}@Sn_{12}^{2-}]$ to $3d^8$ in $[Ni^{2+}@Sn_{12}^{2-}]$, giving rise to a new class of cage clusters with tunable magnetic and optical properties. In contrast to the encapsulated Si or Ge clusters, where the dopants are critical to stabilize the cage structures,[84–91] the stability of $M@Sn_{12}$ derives from the intrinsic stability of stannaspherene itself, much like the endohedral fullerenes. Our study indicates that all the transition metal or f-block atoms can be trapped inside stannaspherene. This is quite advantageous relative to the endohedral fullerenes, which can only trap the alkali, alkali earth, or rare earth atoms while the chemically more interesting transition metal atoms do not form endohedral fullerenes.[83]

5. Bulk synthesis of endohedral stannaspherene

5.1. *Observation of* $Pd_2@Sn_{18}^{4-}$

The high stability of stannaspherene (Sn_{12}^{2-}) and plumbaspherene (Pb_{12}^{2-}) suggests that they may be synthesized in solution and may be crystallized with appropriate counter ions. Eichhorn and co-workers have synthesized a series of endohedral cage compounds, $M@Pb_{12}^{2-}$ (M = Ni, Pd, Pt), through chemical reactions of K_4Pb_9 and ML_4 (M = Pt, Pd, L = PPh_3) in ethylenediamine (ED) and crystallized them as (2,2,2-crypt)K^+ salts.[92–94] Inspired by the Eichhorn compounds, we started exploratory syntheses of endohedral stannaspherenes. Interestingly, we found a new $Pd_2@Sn_{18}^{4-}$ cluster, which has been crystallized as a $[(2,2,2\text{-crypt})K]_4(Pd_2@Sn_{18})\cdot$ 3ED salt during our attempt to synthesize the endohedral stannaspherene $Pd@Sn_{12}^{2-}$.[52] Its structure has been determined by single-crystal X-ray diffraction and the $Pd_2@Sn_{18}^{4-}$ cluster is found to consist of 18 Sn atoms encapsulating two non-bonding Pd atoms and are in fact due to the fusion of two endohedral stannaspherenes ($Pd@Sn_{12}^{2-}$) along their C_3 axis by removing a Sn_3 triangle on each Sn_{12} unit at the cluster-cluster joint.

The $[K(2,2,2\text{-crypt})]_4(Pd_2@Sn_{18})\cdot 3ED$ compound was crystallized in an ED solution via the reaction of K_4Sn_9 and $Pd[P(C_6H_5)_3]_4$. The $Pd_2@Sn_{18}^{4-}$ anion is a *closo*-deltahedral cluster, consisting of 18 Sn atoms encapsulating two Pd atoms. It only has an inversion symmetry, but its overall prolate shape is *pseudo-*D_{3d}. The Pd . . . Pd distance (3.414 Å) is beyond the range of observed single Pd-Pd bond distances (2.53–2.70 Å),[95,96] indicating nonbonding interactions or simply two isolated Pd atoms. The structure of $Pd_2@Sn_{18}^{4-}$ is identical to that of $Pd_2@Ge_{18}^{4-}$ reported previously by Sevov *et al.*[97] However, the Pd-Pd distance (2.831 Å) in $Pd_2@Ge_{18}^{4-}$ indicates a weakly bonded Pd_2 dimer, perhaps imposed by the shorter Ge-Ge distances as suggested by Sevov *et al.* The $Pd_2@Sn_{18}^{4-}$ cluster also bears some similarity to a Pt-Sn cluster ($Pt_2@Sn_{17}^{4-}$) recently reported by Eichhorn and co-workers.[98]

5.2. *The structure and bonding of* $Pd_2@Sn_{18}^{4-}$

The $Pd_2@Sn_{18}^{4-}$ cluster consists of two identical $PdSn_9^{2-}$ units connected by an inversion centre. More importantly, each of the $PdSn_9^{2-}$ unit is part of a $Pd@Sn_{12}^{2-}$ endohedral stannaspherene by removing a Sn_3 triangle with very little structural relaxation

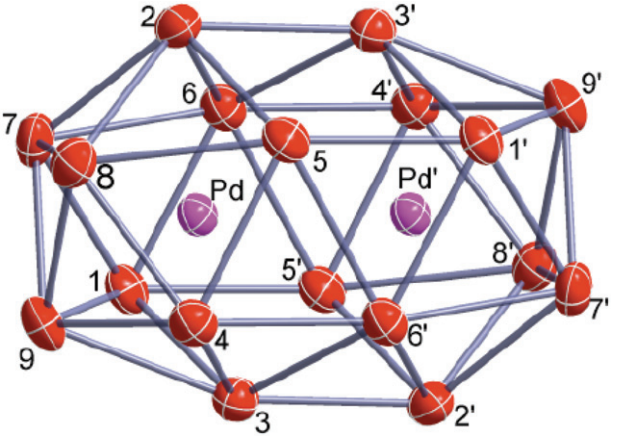

Figure 18. ORTEP view of the structure of $Pd_2@Sn_{18}^{4-}$ in $[K(2,2,2\text{-crypt})]_4$ $(Pd_2@Sn_{18})\cdot 3ED$ (50% thermal ellipsoids). From ref. 52.

(Figure 19c). Thus the $Pd_2@Sn_{18}^{4-}$ cluster can be viewed as the fusion of two endohedral stannaspherenes along their C_3 axis. The Pd-Sn distance is about 2.90 Å within each $PdSn_9^{2-}$ sub-unit, whereas the Sn-Sn distances are in the range of 3.012 to 3.145 Å, which are shorter than the calculated Sn-Sn distance (3.19 Å) for stannaspherene due to the Pd-Sn interactions. Only three Sn-Sn bonds are slightly elongated: Sn(7)-Sn(6), Sn(8)-Sn(5), and Sn(9)-Sn(3), which are probably caused by the fact that Sn(6, 5, 3) have to 'reach out' to bond to the second $Pd'Sn'_9{}^{2-}$ sub-unit (Figure 19b). The six horizontal Sn-Sn bonds, i.e. Sn(1)-Sn(5′), Sn(2)-Sn(3′), Sn(3)-Sn(2′), Sn(4)-Sn(6′), Sn(5)-Sn(1′), and Sn(6)-Sn(4′), which bridge the two $PdSn_9^{2-}$ units, are relatively short and almost identical to each other (3.089–3.106 Å).

To elucidate the stability and the electronic structure of the new $Pd_2@Sn_{18}^{4-}$ cluster, we carried out quasi-relativistic density functional calculations at the PW91/TZ2P level.[52] We optimized the structure of $Pd_2@Sn_{18}^{4-}$ starting from the crystallographically determined structure and also from stacking two ideal $Pd@Sn_{12}^{2-}$ endohedral stannaspherenes by removing a Sn_3 triangle, i.e. from Figure 19c to 19a. Both led to the same and more symmetric D_{3d} species for the free $Pd_2@Sn_{18}^{4-}$ cluster, which is confirmed to be a minimum through vibrational frequency calculations. Molecular orbital analyses reveal that it can be viewed as two neutral Pd atoms trapped inside a polyhedral Sn_{18}^{4-} with a large HOMO-LUMO gap of 1.44 eV (Figure 20) (compared to 1.70 eV for $Pd@Sn_{12}^{2-}$ and 1.66 eV for $Pd_2@Ge_{18}^{4-}$ at the same level of theory), suggesting that it is a highly electronically stable species.

Stannaspherene has been shown to be able to trap all transition metal atoms including the f-block elements, analogous to endohedral fullerenes. Here we further note that the structural evolution from the nearly spherical stannaspherene to the prolate $Pd_2@Sn_{18}^{4-}$ is also reminiscent of that from C_{60} to C_{70}, as illustrated in Figure 21. Further extension of C_{70} can lead to the formation of a single wall carbon nanotube. It is interesting to speculate if the $Pd_2@Sn_{18}^{4-}$ cluster can be further extended to form carbon nanotube-like structures. Preliminary calculations suggest that insertion of up to two $PdSn_6$ units into

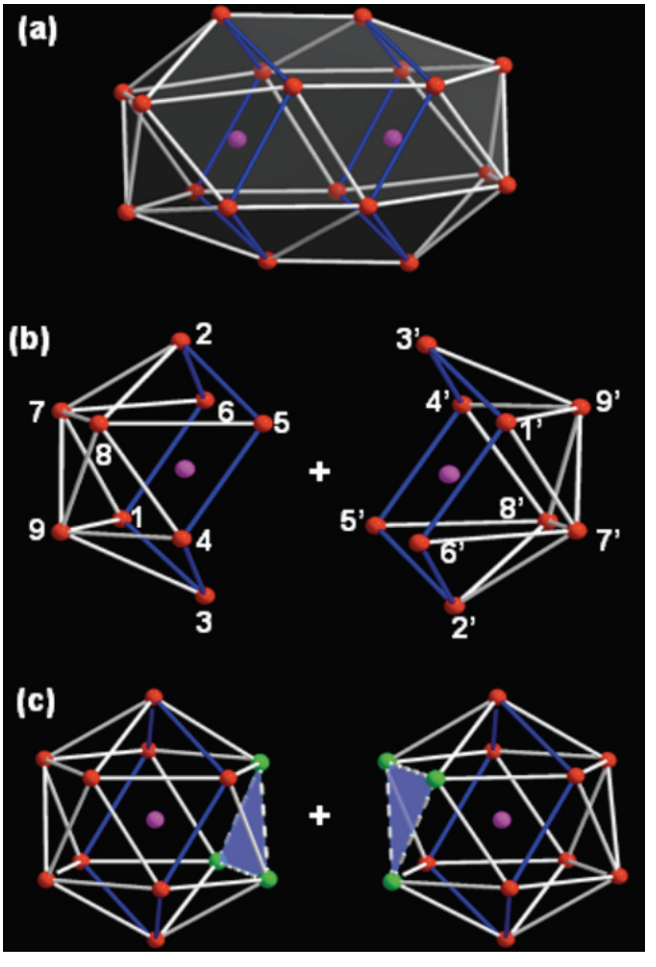

Figure 19. Relationship of $Pd_2@Sn_{18}^{4-}$ and stannaspherene $Pd@Sn_{12}^{2-}$. (a) the $Pd_2@Sn_{18}^{4-}$ cluster, (b) the two halves ($PdSn_9^{2-}$) of $Pd_2@Sn_{18}^{4-}$ separated along its *pseudo*-C_3 axis for clear view, (c) reconstruction of two endohedral stannaspherenes $Pd@Sn_{12}^{2-}$ by adding a Sn_3 triangle (green) to the two $PdSn_9^{2-}$ subunits. From ref. 52.

$Pd_2@Sn_{18}^{4-}$ still lead to stable structures, i.e. both $Pd_3@Sn_{24}^{4-}$ and $Pd_4@Sn_{30}^{6-}$ clusters are stable with reasonable HOMO-LUMO gaps.

Starting from the nine-atom Zintl ions E_9^{x-} (E = Ge, Sn, Pb; $x = 2$–4),[99] several interesting new clusters have been synthesized.[92–94,97,98,100–102] The recent synthesis of the *closo*-Pd_{10}^{2-} cluster[101] from the Pd_9^{4-} Zintl ion suggests that the parent stannaspherene (Sn_{12}^{2-}) and plumbaspherene (Pb_{12}^{2-}) may also be obtained from the respective E_9^{x-} Zintl ions under appropriate reaction conditions. Indeed this work and the previous work on $M@Pb_{12}^{2-}$ and $Pt_2@Pb_{17}^{4-}$, as well as the observation of other possible gaseous Cu-Sn core–shell clusters,[103] suggest that a whole class of endohedral stannaspherenes and plumbaspherenes with various internal atoms, as well as other novel endohedral structures, may be synthesized and crystallized.

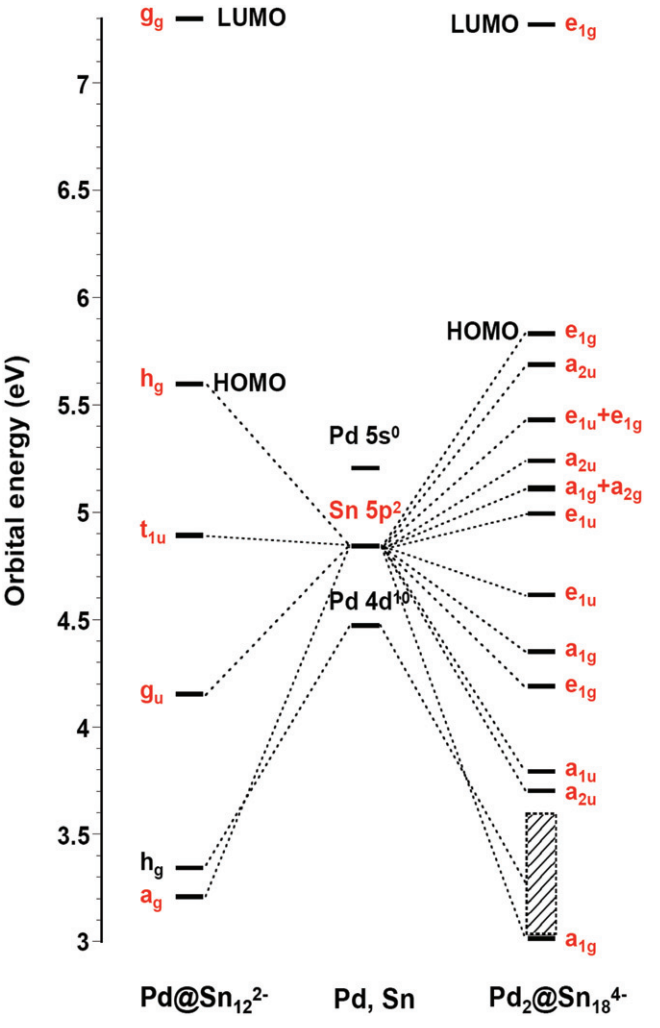

Figure 20. Scalar-relativistic molecular orbital levels of $Pd@Sn_{12}^{2-}$ (I_h) and $Pd_2@Sn_{18}^{4-}$ (D_{3d}). The orbital energies of the Sn and Pd atoms and the $Pd@Sn_{12}^{2-}$ dianion are shifted up to match those of the $Pd_2@Sn_{18}^{4-}$ tetraanion. Note the large HOMO-LUMO gaps for both clusters. From ref. 52.

6. Final remarks and perspectives

Although polyhedral cages are common in inorganic compounds,[104] empty cage clusters with large interior volumes are very rare. Cage structures involving Sn are known in inorganic complexes and the Zintl phases.[105,106] However, the I_h-Sn_{12}^{2-} empty cage is not known before. The high stability of this cluster suggests that it may be synthesized in the solid state using suitable ligands or counter ions. The Sn_{12}^{2-} cage has a diameter of ~6.1 Å, only slightly smaller than that of C_{60} and has been shown to be able to host a variety of atoms, including all the transition metal and f-block atoms, even more versatile than the fullerenes. A prior theoretical calculation has shown that $Cd@Sn_{12}$ is a stable I_h cage.[89]

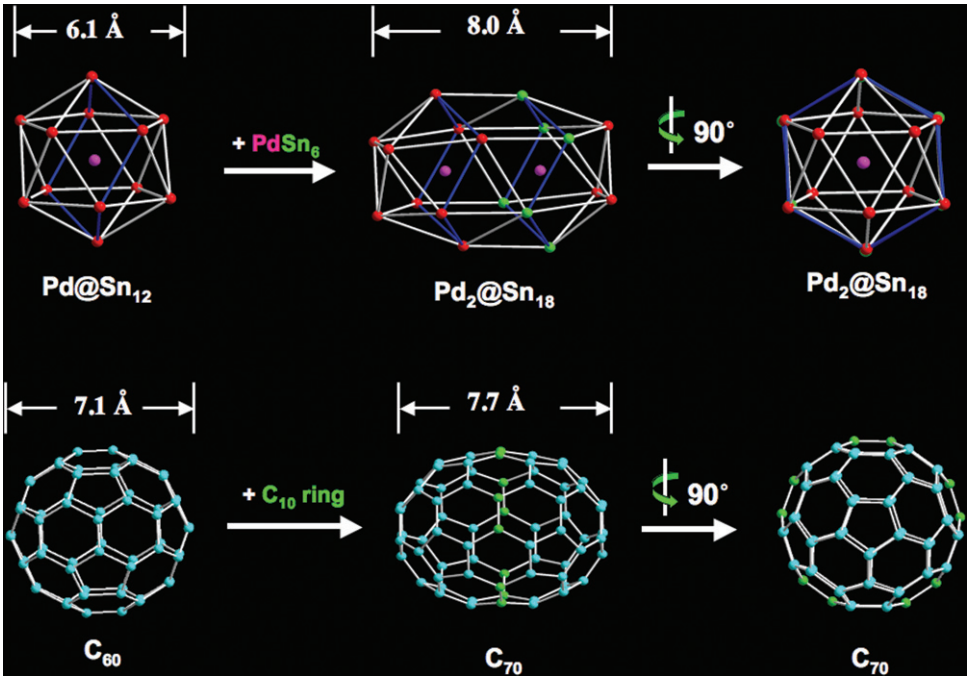

Figure 21. Comparison of the structural evolution from $Pd@Sn_{12}^{2-}$ to $Pd_2@Sn_{18}^{4-}$ to that from C_{60} to C_{70}. From ref. 52.

A recent mass spectrometric study revealed stable Cu-Sn cluster compositions from high-temperature annealing, suggesting larger core-shell type of cage structures.[103] Thus, a whole new family of endohedral stannaspherenes and larger Sn cage clusters may exist.

Plumbaspherene has a diameter slightly larger than that of stannaspherene. Thus, it is also expected that Pb_{12}^{2-} can trap an atom inside to form endohedral plumbaspherenes, $M@Pb_{12}$. Indeed, it has been shown computationally that plumbaspherene can even trap a Pu atom to form a 32-electron endohedral $Pu@Pb_{12}$ cluster,[107] as well as heavier group-13 atoms.[108] In fact, several endohedral $M@Pb_{12}$ clusters have been observed experimentally. A series of $[M@Pb_{12}]^{2-}$ species (M = Pt, Pd, Ni) have been synthesized in solution and crystallized with K^+(2,2,2-crypt) as counter ions.[92–94] X-ray diffraction and NMR experiments have confirmed that these clusters do possess I_h symmetry. They can be viewed as a zero-valent Pt (Pd or Ni) atom trapped inside plumbaspherene, i.e. $M@Pb_{12}^{2-}$. In a laser vaporization experiment involving Pb and Al, a cluster with the composition $AlPb_{12}^+$ was observed to be unusually intense in the mass distribution.[109,110] Density functional calculations show that this cluster possesses an I_h structure with a closed electron shell and it can be viewed as an Al^{3+} ion trapped inside plumbaspherene, $Al^{3+}@Pb_{12}^{2-}$, to give a total charge of +1. In another laser vaporization experiment involving Pb/Co, the $CoPb_{12}^-$ cluster was observed to be relatively intense in the mass distribution and was proposed to be an icosahedral $Co@Pb_{12}$ cage.[111]

A very recent report describes the synthesis of an empty polyhedral Pb_{10}^{2-} cage, which is compared to the $B_{10}H_{10}^{2-}$ borane.[112] Our PES and theoretical investigations suggest that

the Pb_{12}^{2-} plumbaspherene is also highly stable and can be synthesized in the condensed phase. More importantly, our studies imply that the previously observed $M@Pb_{12}$ clusters are all due to the intrinsic stability of the *empty* plumbaspherene, rather than the effect of the dopant atom. Hence, it is expected that a whole new family of stable $M@Pb_{12}$ endohedral clusters should exist, similar to the endohedral stannaspherene family, with $Pt@Pb_{12}^{2-}$ or $Ni@Pb_{12}^{2-}$ or $[Al^{3+}@Pb_{12}^{2-}]$ as specific members of the new family of endohedral plumbaspherenes. Metal-encapsulated Si or Ge clusters have been reported previously.[84–90] Icosahedral $M@Au_{12}$ types of cage clusters have also been predicted[113] and observed experimentally.[114] However, the dopant atoms are critical for these cage structures because the bare Si/Ge clusters or Au_{12} do not possess cage structures.[9] The only other family of empty metallic cages are Au_{16}^{-} and Au_{17}^{-}, which have been found to be hollow cage clusters[13] and can also trap a metal atom inside to form endohedral golden cage clusters.[115] Au_{32} has been proposed as an unprecedented I_h cage cluster on the basis of theoretical calculations,[116,117] but has not been observed or confirmed experimentally.[118]

If flexible bulk synthetic methods can be found for the vast number of endohedral stannaspherenes and plumbaspherenes, we anticipate the creation of novel cluster-assembled materials with continuously tunable electronic, magnetic, or optical properties across the entire transition series or the f-block elements. Our synthesis of $Pd_2@Sn_{18}^{4-}$, due to the fusion of two $Pd@Sn_{12}^{2-}$, and the prior synthesis of $M@Pb_{12}^{2-}$ (M = Pt, Pd, Ni) indicate that a whole class of endohedral stannaspherenes and plumbaspherenes with various internal atoms, as well as other novel endohedral structures, should be able to be synthesized and crystallized. It is also expected that combined experimental and theoretical investigations with increased levels of sophistications will uncover many more interesting and novel clusters, which may be considered as building blocks for cluster-assembled nanomaterials.

Acknowledgements

We would like to thank Prof. A. I Boldyrev, Dr. Xin Huang, Dr. Jun Li, Dr. Zhong-Ming Sun, and Mr. Lei-Ming Wang for their contributions to the works described in this article. This work was supported by the National Science Foundation (DMR-0503383) and partially by the Donors of the Petroleum Fund, administered by the American Chemical Society (PRF# 46275-AC6). All the experiments were performed at the W. R. Wiley Environmental Molecular Sciences Laboratory, a national scientific user facility sponsored by the DOE's Office of Biological and Environmental Research and located at Pacific Northwest National Laboratory, operated for the DOE by Battelle.

References

[1]H.W. Kroto, J.R. Heath, S.C. Obrien, R.F. Curl and R.E. Smalley, Nature **318**, 162 (1985).
[2]W. Kratschmer, L.D. Lamb, K. Fostiropoulos and D.R. Huffman, Nature **347**, 354 (1990).
[3]X. Li, A.E. Kuznetsov, H.F. Zhang, A.I. Boldyrev and L.S. Wang, Science **291**, 859 (2001).
[4]A.E. Kuznetsov, A.I. Boldyrev, X. Li and L.S. Wang, J. Am. Chem. Soc. **123**, 8825 (2001).
[5]H.J. Zhai, A.N. Alexandrova, K.A. Birch, A.I. Boldyrev and L.S. Wang, Angew. Chem. Int. Ed. **42**, 6004 (2003).
[6]H.J. Zhai, B. Kiran, J. Li and L.S. Wang, Nature Materials **2**, 827 (2003).

[7]B. Kiran, S. Bulusu, H.J. Zhai, S. Yoo, X.C. Zeng and L.S. Wang, Proc. Natl. Acad. Sci. (USA) **102**, 961 (2005).
[8]E. Oger, N. R. M. Crawford, R. Kelting, P. Weis, M.M. Kappes and R. Ahlrichs, Angew. Chem. Int. Ed. **46**, 1 (2007).
[9]F. Furche, R. Ahlrichs, P. Weis, C. Jacob, S. Gilb, T. Bierweiler and M.M. Kappes, J. Chem. Phys. **117**, 6982 (2002).
[10]H. Häkkinen, M. Moseler and U. Landman, Phys. Rev. Lett. **89**, 033401 (2002).
[11]H. Häkkinen, B. Yoon, U. Landman, X. Li, H.J. Zhai and L.S. Wang, J. Phys. Chem. A **107**, 6168 (2003).
[12]J. Li, X. Li, H.J. Zhai and L.S. Wang, Science **299**, 864 (2003).
[13]S. Bulusu, X. Li, L.S. Wang and X.C. Zeng, Proc. Natl. Acad. Sci. (USA) **103**, 8326 (2006).
[14]X. Li, H. Wu, X.B. Wang and L.S. Wang, Phys. Rev. Lett. **81**, 1909 (1998).
[15]D.E. Bergeron, A.W. Castleman, T. Morisato and S.N. Khanna, Science **304**, 84 (2004).
[16]X. Li, A. Grubisic, S.T. Stokes, J. Cordes, G.F. Ganteför, K.H. Bowen, B. Kiran, M. Willis, P. Jena, R. Burgert and H. Schnöckel, Science **315**, 356 (2007).
[17]W.L. Brown, R.R. Freeman, K. Raghavachari and M. Schluter, Science **235**, 860 (1987).
[18]M.F. Jarrold, Science **252**, 1085 (1991).
[19]E.C. Honea, A. Ogura, C.A. Murray, K. Raghavachari, W.O. Sprenger, M.F. Jarrold and W. L. Brown, Nature **366**, 42 (1993).
[20]Q.L. Zhang, Y. Liu, R.F. Curl, F.K. Tittel and R.E. Smalley, J. Chem. Phys. **88**, 1670 (1988).
[21]S. Li, R.J. Vanzee, W. Weltner and K. Raghavachari, Chem. Phys. Lett. **243**, 275 (1995).
[22]O. Cheshnovsky, S.H. Yang, C.L. Pettiette, M.J. Craycraft, Y. Liu and R.E. Smalley, Chem. Phys. Lett. **138**, 119 (1987).
[23]C.C. Arnold and D.M. Neumark, J. Chem. Phys. **99**, 3353 (1993).
[24]C.S. Xu, T.R. Taylor, G.R. Burton and D.M. Neumark, J. Chem. Phys. **108**, 1395 (1998).
[25]M. Maus, G. Gantefor and W. Eberhardt, Appl. Phys. A **70**, 535 (2000).
[26]M.A. Hoffmann, G. Wrigge, B. von Issendorff, J. Muller, G. Ganteför and H. Haberland, Eur. Phys. J. D **16**, 9 (2001).
[27]S. Ogut, J.R. Chelikowsky and S.G. Louie, Phys. Rev. Lett. **79**, 1770 (1997).
[28]J. Muller, B. Liu, A.A. Shvartsburg, S. Ogut, J.R. Chelikowsky, K.W.M. Siu, K.M. Ho and G. Gantefor, Phys. Rev. Lett. **85**, 1666 (2000).
[29]J. Bai, L.F. Cui, J.L. Wang, S.H. Yoo, X. Li, J. Jellinek, C. Koehler, T. Frauenheim, L.S. Wang and X.C. Zeng, J. Phys. Chem. A **110**, 908 (2006).
[30]Y. Negishi, H. Kawamata, F. Hayakawa, A. Nakajima and K. Kaya, Chem. Phys. Lett. **294**, 370 (1998).
[31]G.R. Burton, C.S. Xu, C.C. Arnold and D.M. Neumark, J. Chem. Phys. **104**, 2757 (1996).
[32]M.F. Jarrold and J.E. Bower, J. Chem. Phys. **96**, 9180 (1992).
[33]K.M. Ho, A.A. Shvartsburg, B.C. Pan, Z.Y. Lu, C.Z. Wang, J.G. Wacker, J.L. Fye and M.F. Jarrold, Nature **392**, 582 (1998).
[34]J.M. Hunter, J.L. Fye, M.F. Jarrold and J.E. Bower, Phys. Rev. Lett. **73**, 2063 (1994).
[35]A.A. Shvartsburg, B. Liu, Z.Y. Lu, C.Z. Wang, M.F. Jarrold and K.M. Ho, Phys. Rev. Lett. **83**, 2167 (1999).
[36]A.A. Shvartsburg, B. Liu, M.F. Jarrold and K.M. Ho, J. Chem. Phys. **112**, 4517 (2000).
[37]R.R. Hudgins, M. Imai, M.F. Jarrold and P. Dugourd, J. Chem. Phys. **111**, 7865 (1999).
[38]Q. Sun, Q. Wang, P. Jena, S. Waterman and Y. Kawazoe, Phys. Rev. A **67**, 063201 (2003).
[39]S. Yoo, X.C. Zeng, X.L. Zhu and J. Bai, J. Am. Chem. Soc. **125**, 13318 (2003).
[40]S. Yoo, J.J. Zhao, J.L. Wang and X.C. Zeng, J. Am. Chem. Soc. **126**, 13845 (2004).
[41]S.H. Yoo and X.C. Zeng, Angew. Chem. Int. Ed. **44**, 1491 (2005).
[42]S. Ogut and J.R. Chelikowsky, Phys. Rev. B **55**, R4914 (1997).
[43]J.L. Wang, G.H. Wang and J.J. Zhao, Phys. Rev. B **64**, 205411 (2001).
[44]S. Bulusu, S. Yoo and X.C. Zeng, J. Chem. Phys. **122**, 164305 (2005).

[45]D.K. Yu, R.Q. Zhang and S.T. Lee, Phys. Rev. B **65**, 245417 (2002).
[46]Q. Sun, Q. Wang, P. Jena, B.K. Rao and Y. Kawazoe, Phys. Rev. Lett. **90**, 135503 (2003).
[47]A.A. Shvartsburg and M.F. Jarrold, Phys. Rev. A **60**, 1235 (1999).
[48]A.A. Shvartsburg and M.F. Jarrold, Chem. Phys. Lett. **317**, 615 (2000).
[49]L.F. Cui, X. Huang, L.M. Wang, D.Y. Zubarev, A.I. Boldyrev, J. Li and L.S. Wang, J. Am. Chem. Soc. **128**, 8390 (2006).
[50]L.F. Cui, X. Huang, L.M. Wang, J. Li and L.S. Wang, J. Phys. Chem. A **110**, 10169 (2006).
[51]L.F. Cui, X. Huang, L.M. Wang, J. Li and L.S. Wang, Angew. Chem. Int. Ed. **46**, 742 (2007).
[52]Z.M. Sun, H. Xiao, J. Li and L.S. Wang, J. Am. Chem. Soc. **129**, 9560 (2007).
[53]A.I. Boldyrev and L.S. Wang, J. Phys. Chem. A **105**, 10759 (2001).
[54]A.I. Boldyrev and L.S. Wang, Chem. Rev. **105**, 3716 (2005).
[55]A.N. Alexandrova, A.I. Boldyrev, H.J. Zhai and L.S. Wang, Coord. Chem. Rev. **250**, 2811 (2006).
[56]H.J. Zhai and L.S. Wang, in *The Chemical Physics of Solid Surfaces. Atomic Clusters from Gas Phase to Deposited*. edited by D.P. Woodruff (Elsevier, New York, 2007), Vol. 12, pp. 91–150.
[57]L.S. Wang, H.S. Cheng, and J. Fan, J. Chem. Phys. **102**, 9480 (1995); L.S. Wang and H. Wu, in Advances in Metal and Semiconductor Clusters. IV. Cluster Materials. Ed. M.A. Duncan, JAI Press, Greenwich (1998), pp. 299–343.
[58]J. Akola, M. Manninen, H. Hakkinen, U. Landman, X. Li and L.S. Wang, Phys. Rev. B **60**, 11297 (1999).
[59]L.S. Wang and X. Li, in *Clusters and Nanostructure Interfaces*. edited by P. Jena, S.N. Khanna, and B.K. Rao (World Scientific, River Edge, New Jersey, 2000), pp. 293–300.
[60]W.G. Burgers and L.J. Groen, Faraday Soc. Discuss. **23**, 183 (1957).
[61]A.A. Shvartsburg and M.F. Jarrold, Phys. Rev. Lett. **85**, 2530 (2000).
[62]T.P. Martin and H. Schaber, J. Chem. Phys. **83**, 855 (1985).
[63]K. Laihing, R.G. Wheeler, W.L. Wilson and M.A. Duncan, J. Chem. Phys. **87**, 3401 (1987).
[64]S. Yoshida and K. Fuke, J. Chem. Phys. **111**, 3880 (1999).
[65]Z.Y. Lu, C.Z. Wang and K.M. Ho, Phys. Rev. B **61**, 2329 (2000).
[66]C. Majumder, V. Kumar, H. Mizuseki and Y. Kawazoe, Phys. Rev. B **64**, 233405 (2001).
[67]K. Joshi, D.G. Kanhere and S.A. Blundell, Phys. Rev. B **67**, 235413 (2003).
[68]F.C. Chuang, C.Z. Wang, S. Ogut, J.R. Chelikowsky and K.M. Ho, Phys. Rev. B **69**, 165408 (2004).
[69]G. Ganteför, M. Gausa, K.H. Meiwesbroer and H.O. Lutz, Z. Phys. D **12**, 405 (1989).
[70]V.D. Moravec, S.A. Klopcic and C.C. Jarrold, J. Chem. Phys. **110**, 5079 (1999).
[71]Y. Negishi, H. Kawamata, A. Nakajima and K. Kaya, J. Electron. Spectrosc. Relat. Phenom. **106**, 117 (2000).
[72]L.F. Cui, L.M. Wang and L.S. Wang, J. Chem. Phys. **126**, 064505 (2007).
[73]H.C. Longuet-Higgins and M. d. V. Roberts, Proc. Roy. Soc. A **230**, 110 (1955).
[74]A.R. Pitochelli and M.F. Hawthorne, J. Am. Chem. Soc. **82**, 3228 (1960).
[75]P. Pyykkö, Chem. Rev. **88**, 563 (1988).
[76]S.K. Lai, P.J. Hsu, K.L. Wu, W.K. Liu and M. Iwamatsu, J. Chem. Phys. **117**, 10715 (2002).
[77]J. P. K. Doye and S.C. Hendy, Eur. Phys. J. D **22**, 99 (2003).
[78]B.L. Wang, J.J. Zhao, X.S. Chen, D.N. Shi and G.H. Wang, Phys. Rev. A **71** (2005).
[79]C. Rajesh, C. Majumder, M. G. R. Rajan and S.K. Kulshreshtha, Phys. Rev. B **72** (2005).
[80]Y. Chai, T. Guo, C.M. Jin, R.E. Haufler, L. P. F. Chibante, J. Fure, L.H. Wang, J.M. Alford and R.E. Smalley, J. Phys. Chem. **95**, 7564 (1991).
[81]D.S. Bethune, R.D. Johnson, J.R. Salem, M.S. Devries and C.S. Yannoni, Nature **366**, 123 (1993).
[82]W. Plass, H. Stoll, H. Preuss and A. Savin, J. Mol. Struct. (Theochem) **339**, 67 (1995).
[83]T. Guo, R.E. Smalley and G.E. Scuseria, J. Chem. Phys. **99**, 352 (1993).
[84]S.M. Beck, J. Chem. Phys. **87**, 4233 (1987).
[85]H. Hiura, T. Miyazaki and T. Kanayama, Phys. Rev. Lett. **86**, 1733 (2001).
[86]V. Kumar and Y. Kawazoe, Phys. Rev. Lett. **8704**, 045503 (2001).

[87]S.N. Khanna, B.K. Rao and P. Jena, Phys. Rev. Lett. **89**, 016803 (2002).
[88]K. Koyasu, M. Akutsu, M. Mitsui and A. Nakajima, J. Am. Chem. Soc. **127**, 4998 (2005).
[89]V. Kumar and Y. Kawazoe, Appl. Phys. Lett. **80**, 859 (2002).
[90]V. Kumar, A.K. Singh and Y. Kawazoe, Nano Lett. **4**, 677 (2004).
[91]C. Schrodt, F. Weigend and R. Ahlrichs, Z. Anorg. Allg. Chem. **628**, 2478 (2002).
[92]E.N. Esenturk, J. Fettinger and B. Eichhorn, J. Am. Chem. Soc. **128**, 9178 (2006).
[93]E.N. Esenturk, J. Fettinger and B. Eichhorn, Chem. Comm. **247** (2005).
[94]E.N. Esenturk, J. Fettinger, Y.F. Lam and B. Eichhorn, Angew. Chem. Int. Ed. **43**, 2132 (2004).
[95]R. Vilar, D. M. P. Mingos and C.J. Cardin, J. Chem. Soc. Dalton Trans. **4313** (1996).
[96]J. Vicente, J.A. Abad, A.D. Frankland, J. Lopez-Serrano, M. C. R. de Arellano and P.G. Jones, Organometallics **21**, 272 (2002).
[97]J.M. Goicoechea and S.C. Sevov, J. Am. Chem. Soc. **127**, 7676 (2005).
[98]B. Kesanli, J.E. Halsig, P. Zavalij, J.C. Fettinger, Y.F. Lam and B.W. Eichhorn, J. Am. Chem. Soc. **129**, 4567 (2007).
[99]J.D. Corbett, Chem. Rev. **85**, 383 (1985).
[100]T.F. Fässler and S.D. Hoffmann, Angew. Chem. Int. Ed. **43**, 6242 (2004).
[101]A. Spiekermann, S.D. Hoffmann and T.F. Fässler, Angew. Chem. Int. Ed. **45**, 3459 (2006).
[102]J.M. Goicoechea and S.C. Sevov, J. Am. Chem. Soc. **128**, 4155 (2006).
[103]G.A. Breaux, D.A. Hillman, C.M. Neal and M.F. Jarrold, J. Phys. Chem. A **109**, 8755 (2005).
[104]S. Alvarez, Dalton Trans. **2209** (2005).
[105]N. Wiberg and P. Power, in *Molecular Clusters of the Main Group Elements*. edited by M. Driess and H. Nöth (WILEY-VCH Verlag, Weinheim, 2004), pp. 188–208.
[106]J.D. Corbett, Angew. Chem. Int. Ed. **39**, 670 (2000).
[107]J.-P. Dognon, C. Clavaguéra and P. Pyykkö, Angew. Chem. Int. Ed. **46**, 1427 (2007).
[108]D.-L. Chen, W.Q. Tian, W.-C. Lu and C.-C. Sun, J. Chem. Phys. **124**, 154313 (2006).
[109]S. Neukermans, E. Janssens, Z.F. Chen, R.E. Silverans, P. v. R. Schleyer and P. Lievens, Phys. Rev. Lett. **92**, 163401 (2004).
[110]Z.F. Chen, S. Neukermans, X. Wang, E. Janssens, Z. Zhou, R.E. Silverans, R.B. King, P.v.R. Schleyer and P. Lievens, J. Am. Chem. Soc. **128**, 12829 (2006).
[111]X. Zhang, G.L. Li, X.P. Xing, X. Zhao, Z.C. Tang and Z. Gao, Rapid Commun. Mass Spectrom. **15**, 2399 (2001).
[112]A. Spiekermann, S.D. Hoffinann and T.F. Fässler, Angew. Chem. Int. Ed. **45**, 3459 (2006).
[113]P. Pyykkö and N. Runeberg, Angew. Chem. Int. Ed. **41**, 2174 (2002).
[114]X. Li, B. Kiran, J. Li, H.J. Zhai and L.S. Wang, Angew. Chem. Int. Ed. **41**, 4786 (2002).
[115]L.M. Wang, S. Bulusu, H.J. Zhai, X.C. Zeng and L.S. Wang, Angew. Chem. Int. Ed. **46**, 2915 (2007).
[116]M.P. Johansson, D. Sundholm and J. Vaara, Angew. Chem. Int. Ed. **43**, 2678 (2004).
[117]X. Gu, M. Ji, S.H. Wei and X.G. Gong, Phys. Rev. B **70**, 205401 (2004).
[118]M. Ji, X. Gu, X. Li, X.G. Gong, J. Li and L.S. Wang, Angew. Chem. Int. Ed. **44**, 7119 (2005).